HTL TR NO. 101

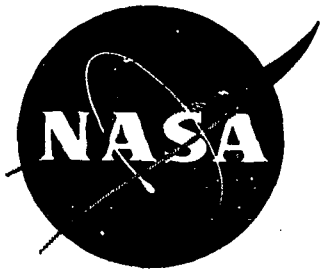

A MODEL FOR ANALYSIS OF THE TEMPERATURE FIELD DOWNSTREAM OF A HEATED JET INJECTED INTO AN ISOTHERMAL CROSSFLOW AT AN ANGLE OF 90°

V. L. Eriksen,

E. R. G. Eckert,

R. J. Goldstein

prepared for

NATIONAL AERONAUTICS AND SPACE ADMINISTRATION

NASA CONTRACT NO. NAS 3-13200

HEAT TRANSFER LABORATORY

MECHANICAL ENGINEERING DEPARTMENT

UNIVERSITY OF MINNESOTA

NOTICE

This report was prepared as an account of Government sponsored work. Neither the United States, nor the National Aeronautics and Space Administration (NASA), nor any person acting on behalf of NASA:

A.) Makes any warranty or representation, expressed or implied, with respect to the accuracy, completeness, or usefulness of the information contained in this report, or that the use of any information, apparatus, method, or process disclosed in this report may not infringe privately owned rights; or

B.) Assumes any liabilities with respect to the use of, or for damages resulting from the use of any information, apparatus, method or process disclosed in this report.

As used above, "person acting on behalf of NASA" includes any employee or contractor of NASA, or employee of such contractor, to the extent that such employee or contractor of NASA, or employee of such contractor prepares, disseminates, or provides access to, any information pursuant to his employment or contract with NASA, or his employment with such contractor.

Requests for copies of this report should be referred to:

National Aeronautics and Space Administration
Office of Scientific and Technical Information
P. O. Box 33
College Park, Maryland 20740

NASA CR-72990
HTL TR NO. 101

SUMMARY REPORT

A MODEL FOR ANALYSIS OF THE TEMPERATURE FIELD DOWNSTREAM OF A HEATED JET INJECTED INTO AN ISOTHERMAL CROSSFLOW AT AN ANGLE OF 90°

by

V. L. Eriksen, E.R.G. Eckert, and R. J. Goldstein

prepared for

NATIONAL AERONAUTICS AND SPACE

ADMINISTRATION

July 1971

CONTRACT NAS 3-13200
TECHNICAL MANAGEMENT
NASA Lewis Research Center
Cleveland, Ohio
Lewis Project Manager; Francis S. Stepka

University of Minnesota
Institute of Technology
Department of Mechanical Engineering
Minneapolis, Minnesota 55455

ABSTRACT

The temperature distribution downstream of a heated jet entering an isothermal crossflow at an angle of 90^{o} is predicted using two conduction models with energy sources above the point of injection, in one case a point source and in the second a line source. The models use effective turbulent diffusivities that are determined empirically from previous measurements. Temperatures predicted by the models are compared to experimental results.

NOMENCLATURE

c_p	specific heat at constant pressure per unit mass
D	diameter of injection tube
k	thermal conductivity
M	blowing rate parameter, $\rho_2 U_2 / \rho_\infty U_\infty$
$\dot{q}$	strength of line source per unit length
$\dot{Q}$	strength of energy source and enthalpy flow through injection hole; energy/time
T	temperature
T_{aw}	adiabatic wall temperature
T_m	maximum temperature of (y direction) profile
T_2	temperature of injected air
T_∞	mainstream temperature
U	velocity
U_2	average velocity of secondary flow
U_∞	mainstream velocity
X	distance downstream from center of injection hole, see Figure 1
X_o	component of distance from center of injection hole to energy source in X direction
Y	distance normal to wall through which injected air flows, see Figure 1
Y_o	component of distance from center of injection hole to energy source in Y direction

Z lateral distance from center of injection hole, see Figure 1

Z_o component of distance from center of injection hole to energy source in Z direction

α molecular thermal diffusivity = $\frac{k}{\rho c_p}$

δ boundary layer thickness

ε turbulent thermal diffusivity

ε_ℓ turbulent thermal diffusivity for line source model

ε_p turbulent thermal diffusivity for point source model

$\bar{\varepsilon}$ average turbulent thermal diffusivity

η film cooling effectiveness, defined by Equation 2

θ temperature difference, $T-T_\infty$

θ_m maximum temperature difference, T_m-T_∞

θ_2 injection temperature difference, T_2-T_∞

ν kinematic viscosity

ρ density

ρ_2 density of injected air

ρ_∞ density of mainstream

A MODEL FOR ANALYSIS OF THE TEMPERATURE FIELD DOWNSTREAM OF A HEATED JET INJECTED INTO AN ISOTHERMAL CROSSFLOW AT AN ANGLE OF 90°

by

V. L. Eriksen, E.R.G. Eckert, and R. J. Goldstein

University of Minnesota

I. SUMMARY

The study described in this report is part of an investigation into film cooling following ejection of a secondary gas through discrete holes into a turbulent boundary layer of air on a flat plate. Two models to predict film cooled temperatures are described and their predictions are compared to previous measurements.

The models are based on conduction solutions for a point and a line source of energy moving in an infinite medium. The influence of blowing rate is accounted for by positioning the sources above the point of injection. The turbulent flow characteristics are considered by replacing the molecular thermal diffusivity as it appears in the conduction solution by an effective average turbulent thermal diffusivity. This effective turbulent diffusivity is evaluated by matching the conduction solutions to experimental results for a heated jet injected into an isothermal crossflow at an angle of 90°.

The point source model adequately predicts the temperature along the centerline downstream of injection but not at lateral positions. The line source model takes into account the finite width of the injection hole and is a better representation than the point source model for determining off-centerline temperature. It does not, however, predict centerline temperature quite as well as the point source model.

II. INTRODUCTION

Film cooling is used extensively in various modern devices. As a consequence, a large body of literature is concerned with the prediction of the effectiveness of this cooling method. It deals, however, almost exclusively with ejection of the coolant through openings which are uninterrupted in the direction normal to the main flow. This arrangement creates a temperature field in the fluid downstream of the openings which is two-dimensional, having the same characteristic in all planes normal to the film cooled surface and paralled to the main flow direction.

In various applications, design considerations require that the openings for the ejection of the coolant be interrupted or that they consist of rows of holes. That is, for instance, the case for the film cooling of gas turbine blades. In such an arrangement, the temperature field in the fluid downstream of the openings is three-dimensional and the temperature on

the film cooled surface is two-dimensional. The number of geometries in such an arrangement is almost unlimited because the shape of the openings, their mutual distance, and the direction in which the coolant is ejected can all vary; several rows at various positions along the flow direction may also be considered. The cooling effectiveness created by such an arrangement will depend on the dimensionless parameters describing the main flow as well as the flow of the coolant as it leaves the openings. A test program which covers these parameters becomes therefore very extensive. Predicting the film cooling performance would be simplified if the information could be restricted to average temperatures. Design calculations require, however, the knowledge of the complete temperature field at the film cooled surface. Under these circumstances it is desirable to have an analytical model available which describes the film cooling process at least qualitatively and which, in addition, can be used to interpolate between the test points. Such a model was suggested in reference 1 and proved in the meantime its usefulness for two-dimensional film cooling. An analogous model is described in reference 2 for three-dimensional film cooling. It replaces the ejection of the coolant through a hole by a point energy sink. With the additional assumption that the variation of the properties involved in the cooling process can be neglected, the law of super-position can be applied to the energy sink model and all possible coolant configurations--

like one row or several rows of holes or interrupted slots--can be modeled by super-position of such point heat sinks. It was shown in reference 2 that the energy sink model approximates experimental results for normal ejection of air through a circular hole into a turbulent air boundary layer satisfactorily as long as the ratio of the mass velocity with which the coolant leaves the opening to the mass velocity of the mainstream is small. The present report proposes an extension of this model which leads to an improved approximation of the actual conditions for larger ratios of the mass velocities. It also compares the predictions obtained with this model with experimental results.

The study is specifically concerned with the configuration shown in Figure 1. A jet of density ρ_2, temperature T_2, and mean velocity U_2 enters a main flow of density ρ_∞, and mainstream velocity U_∞. The angle between the axis of the entering jet and the direction of the free stream does not appear as parameter in the analysis. In the experiments to which the analytical results will be compared it is 90°. The hole through which the jet flows is flush with the surface that is to be protected. A turbulent boundary layer of thickness δ is present at the location of the hole. The wall downstream of the hole is postulated to be adiabatic in the sense that the heat flux from the fluid to the surface is zero. The adiabatic wall temperature which this surface assumes is of interest in itself and has also been demonstrated to be a useful

parameter for conditions in which a heat flux is generated either by conduction into the wall or by radiation from the wall surface.

It is well established that heat transfer relations have the same form for the situations in which the fluid ejected through the hole has a higher or lower temperature than the mainstream fluid. The experiments to which the analysis in this report will be compared have been performed with the temperature T_2 larger than T_∞. Therefore, the analytical models will, from here on, consider energy sources.

Temperatures in the flow field will be represented in dimensionless form

$$\frac{\theta}{\theta_2} = \frac{T-T_\infty}{T_2-T_\infty} \tag{1}$$

The adiabatic wall temperatures are described by the film cooling effectiveness

$$\eta = \frac{T_{aw}-T_\infty}{T_2-T_\infty} \tag{2}$$

The following parameters will be used to describe the temperature distribution in the flow and the film cooling effectiveness: The free stream Reynolds number, $Re_\infty = \frac{U_\infty D}{\nu}$, the mass velocity ratio or blowing rate M ($M = \rho_2 U_2/\rho_\infty U_\infty$), and the thickness δ of the boundary layer approching the jet. The density ratio ρ_2/ρ_∞ is specified as close to unity in the analysis and was approximately 0.85 in the experiments, the results of which are used in this paper.

III. POINT ENERGY SOURCE ABOVE THE CENTER OF INJECTION

Measurements of the temperature field downstream of the point of injection as well as flow visualization have demonstrated that the flow ejected from a hole into a mainstream separates from the surface when the blowing rate exceeds a certain value ($M \sim 0.4 - 0.5$). The model described in this section accounts for this fact in the way that a point energy source* is located some distance above the center of the secondary fluid injection hole (Figure 2a). In developing this model we start with an equation which describes the temperature distribution downstream of an energy source of strength $\dot{Q}$, located at X_o, Y_o, Z_o, with an infinite medium moving in steady uniform flow past the source in the positive X direction with velocity U_∞ (reference 3).

$$\theta(X,Y,Z) = \frac{\dot{Q} \exp\left\{-\frac{U_\infty}{2\alpha}\left[\left|\sqrt{(X-X_o)^2 + (Y-Y_o)^2 + (Z-Z_o)^2}\right| - (X-X_o)\right]\right\}}{4\pi k \sqrt{(X-X_o)^2 + (Y-Y_o)^2 + (Z-Z_o)^2}} \quad (3)$$

For the system shown in Figure 2(a), the source is located directly above the center of injection with $X_o = 0$ and $Z_o = 0$. Equation 3 thus simplifies to

$$\theta(X,Y,Z) = \frac{\dot{Q} \exp\left\{-\frac{U_\infty}{2\alpha}\left[\left|\sqrt{X^2 + (Y-Y_o)^2 + Z^2}\right| - X\right]\right\}}{4\pi k \sqrt{X^2 + (Y-Y_o)^2 + Z^2}} \quad (4)$$

*Although the term "heat source" (or sink) is often used in conduction models, "energy source" is actually a more general term.

If the calculation is restricted to the region where X is large compared to $Y-Y_o$ and Z, then

$$\sqrt{X^2 + (Y-Y_o)^2 + Z^2} \simeq X$$

and

$$\sqrt{X^2 + (Y-Y_o)^2 + Z^2} - X \simeq \frac{(Y-Y_o)^2}{2X} + \frac{Z^2}{2X}$$

for $X > 0$. The equation for the temperature distribution in this region is now

$$\theta(X,Y,Z) = \frac{\dot{Q} \exp\left\{-\frac{U_\infty}{4\alpha X}\left[(Y-Y_o)^2 + Z^2\right]\right\}}{4\pi k X} \qquad (5)$$

The strength of the point source is equated to the enthalpy transport $\dot{Q}$ due to mass injection

$$\dot{Q} = \rho_\infty U_\infty M \frac{\pi D^2}{4} \bar{c}_{p_2} \theta_2 \qquad (6)$$

Assuming $c_{p_2} = c_{p_\infty}$, equation (5) can now be written

$$\frac{\theta(X,Y,Z)}{\theta_2} = \frac{MU_\infty D}{16\alpha\frac{X}{D}} \exp\left\{-\frac{U_\infty D}{4\alpha\frac{X}{D}}\left[\left(\frac{Y-Y_o}{D}\right)^2 + \left(\frac{Z}{D}\right)^2\right]\right\} \qquad (7)$$

Equation 7 has to be adapted to the film cooling process in which the secondary fluid is injected into a turbulent boundary layer. This can be done to a first approximation if the thermal diffusivity α is replaced by a turbulent

diffusivity ε_p. This neglects the local variation of the thermal diffusivity in the boundary layer and assumes a homogeneous and isotropic field of turbulence. Wieghardt (Reference 4) and Malhotra and Cermak (Reference 5) have investigated experimentally heat and mass transfer respectively from a point heat and mass source into a turbulent boundary layer. They use relations similar to Equation 5 to correlate their experimental results.

There is another adjustment which has to be made so that the energy source model matches the boundary conditions on an adiabatic wall. This can be done by the method of images. For this purpose, the solution for another source at $Y = -Y_o$ is added to Equation 7. This results in the equation

$$\frac{\theta(X,Y,Z)}{\theta_2} = \frac{MU_\infty D}{16\varepsilon_p \frac{X}{D}} \exp\left\{ - \frac{U_\infty D}{4\varepsilon_p \frac{X}{D}} \left[\left(\frac{Y-Y_o}{D} \right)^2 + \left(\frac{Z}{D} \right)^2 \right] \right\} + \frac{MU_\infty D}{16\varepsilon_p \frac{X}{D}} \exp\left\{ - \frac{U_\infty D}{4\varepsilon_p \frac{X}{D}} \left[\left(\frac{Y+Y_o}{D} \right)^2 + \left(\frac{Z}{D} \right)^2 \right] \right\} \quad (8)$$

To use Equation 8, the distance Y_o at which the heat source is located above the surface and the turbulent diffusivity ε_p have to be determined. The following procedure is proposed: determine the average value, Y_m, of the distance to the temperature maximum above the surface (see Figure 1) for those

values X and Y for which measurements are available within the range for which interpolation is desired. The arithmetic mean of these values Y_m is interpreted as Y_o. In general, measured values of the film cooling effectiveness are used to determine the turbulent diffusivity ε_p. The film cooling effectiveness η is equal to the temperature ratio θ/θ_2 for $Y = 0$. Rearranging Equation 8 yields for this condition

$$\varepsilon_p = \frac{MU_\infty D}{8\eta(X,Z)\frac{X}{D}} \exp\left\{ - \frac{U_\infty D}{4\varepsilon_p \frac{X}{D}}\left[\left(\frac{Y_o}{D}\right)^2 + \left(\frac{Z}{D}\right)^2\right]\right\} \qquad (9)$$

This equation must be solved by iteration because the turbulent diffusivity appears on both sides. It is proposed to calculate turbulent diffusivities with Equation 9 for those locations for which adiabatic wall temperature data are available within the range selected for interpolation, to determine the arithmetic mean of these diffusivities, and to use the mean in Equation 8. Although single values of $\bar{\varepsilon}_p$ and Y_o are used to predict η over the whole test surface, local values could be determined for interpolation.

For very large blowing rates, the values of the film cooling effectiveness are small and generally available with moderate accuracy only. An alternative procedure for determining ε_p can then be based on the maximum temperature T_m (Figure 1). Evaluating Equation 8 at that location leads to

$$\varepsilon_p = \frac{MU_\infty D}{16\frac{\theta}{\theta_2}\Big|_m \frac{X}{D}} \left\{1 + \exp\left[-\frac{U_\infty D}{\varepsilon_p \frac{X}{D}}\left(\frac{Y_m}{D}\right)^2\right]\right\} \qquad (10)$$

which can be used in the same way as Equation 9 to obtain an average value of the turbulent diffusivity for insertion back into Equation 8, which will be used as an interpolation formula.

IV. LINE HEAT SOURCE ABOVE THE POINT OF INJECTION

If the model is used to simulate injection of a secondary fluid through a hole of finite diameter, it can be suspected and it is verified by the calculations in the latter part of this report that the point heat source underestimates the lateral spreading of the temperature. This raises the question whether the analytical model can be improved without making the analysis too unwieldy and suggests the following extension. A line source with a length D extending in the lateral direction Z is arranged at the location of the hole as shown in Figure 2b. The strength $\dot{q}$ per unit length of the line source is postulated constant. The total strength of the line source has to be the same as the enthalpy input $\dot{Q}$ due to mass injection. Thus, from Equation 6

$$\dot{Q} = \rho_\infty U_\infty M \frac{\pi D^2}{4} c_{p2} \theta_2 = \int_{-.5D}^{.5D} \dot{q} dZ = \dot{q} D \qquad (11)$$

The equation for the temperature distribution downstream of the model is derived by considering Equation 5 for a point source ($\dot{q}dZ_o$) that is located at Y_o, Z_o.

$$\theta(X,Y,Z) = \frac{\dot{q}dZ_o}{4\pi kX} \exp\left\{-\frac{U_\infty}{4\alpha X}\left[(Y-Y_o)^2 + (Z-Z_o)^2\right]\right\} \qquad (12)$$

The strength $\dot{q}$ is obtained from Equation 11 and the temperature distribution downstream of a line source is then obtained by integration over the length of the source

$$\theta(X,Y,Z) = \int_{-.5}^{.5} \frac{\rho_\infty U_\infty MDC_{p2}\theta_2}{16k\frac{X}{D}} \exp\left\{-\frac{U_\infty D}{4\alpha\frac{X}{D}}\left[\left(\frac{Y-Y_o}{D}\right)^2 + \left(\frac{Z-Z_o}{D}\right)^2\right]\right\} d\left(\frac{Z_o}{D}\right) \qquad (13)$$

Assuming $c_{p2} = c_{p\infty}$ and carrying out the integration yields,

$$\frac{\theta(X,Y,Z)}{\theta_2} = \left\{\frac{M\sqrt{\pi}}{16}\sqrt{\frac{U_\infty D}{\alpha\frac{X}{D}}} \exp\left[-\frac{U_\infty D}{4\alpha\frac{X}{D}}\left(\frac{Y-Y_o}{D}\right)^2\right]\right\} x$$

$$\left\{\operatorname{erf}\left[\frac{1}{2}\sqrt{\frac{U_\infty D}{\alpha\frac{X}{D}}}\left(\frac{Z}{D} + 0.5\right)\right] - \operatorname{erf}\left[\frac{1}{2}\sqrt{\frac{U_\infty D}{\alpha\frac{X}{D}}}\left(\frac{Z}{D} - 0.5\right)\right]\right\} \qquad (14)$$

The adiabatic boundary condition at the wall is satisfied by the addition of an image line source at $Y = -Y_o$ and the turbulent flow characteristics are considered by replacing the molecular thermal diffusivity with a constant, isotropic, turbulent diffusivity ε_ℓ. The resulting expression for the temperature distribution in the turbulent flow above the adiabatic wall and downstream of the line energy source is

$$\frac{\theta(X,Y,Z)}{\theta_2} = \frac{M\sqrt{\pi}}{16}\sqrt{\frac{U_\infty D}{\varepsilon_\ell \frac{X}{D}}}\left\{\exp\left[-\frac{U_\infty D}{4\varepsilon_\ell \frac{X}{D}}\left(\frac{Y-Y_o}{D}\right)^2\right] + \exp\left[-\frac{U_\infty D}{4\varepsilon_\ell \frac{X}{D}}\left(\frac{Y+Y_o}{D}\right)^2\right]\right\} \times$$

$$\left\{\operatorname{erf}\left[\frac{1}{2}\sqrt{\frac{U_\infty D}{\varepsilon_\ell \frac{X}{D}}}\left(\frac{Z}{D} + 0.5\right)\right] - \operatorname{erf}\left[\frac{1}{2}\sqrt{\frac{U_\infty D}{\varepsilon_\ell \frac{X}{D}}}\left(\frac{Z}{D} - 0.5\right)\right]\right\} \quad (15)$$

The distance Y_o of the line heat source from the wall and the turbulent diffusivity ε_ℓ can be determined in the same way as for the point heat source to use in the interpolation formula (Equation 15).

V. COMPARISON WITH EXPERIMENTAL RESULTS

The Point Source Model

It is important to investigate to what degree the trends in the temperature field and the film cooling effectiveness obtained by the proposed models agree with the results of measurements. Such a comparison will be presented in this section for the point energy source model and in the following section for the line energy source model. Extensive experimental results for film cooling effectiveness with injection through a circular hole are described in Reference 6 and results describing the temperature field in the fluid in Reference 7. The data for normal injection contained therein will be used in the present comparison.

The temperature profiles of Reference 7 were used to determine Y_o. The distance Y_m from the peak of the temperature profile (see Figure 1) to the wall was obtained from the reference for profiles at X/D = 3.56, 5.48, and 10.57, and Z/D = 0.0, 0.25, and 0.50. The arithmetic average of these values at a given M is assumed to be Y_o. The result is presented in Figure 3. It can be observed that the distance at which the source has to be located above the wall increases with blowing rate due to increased jet penetration. Effectiveness data from Reference 6 were used to determine ε_p. For sets of values of M and U_∞, Reference 6 gives an array of effectiveness values in the area $1.3<X/D<42$ and $0.0\leq Z/D\leq 1.5$. Equation 9 was applied to each point in this area. The values of Y_o/D needed for the calculation were taken from Figure 3. Since the model was formulated for the region $X/D>>Z/D$, the iteration scheme to solve Equation 9 did not converge in the area where X/D is not large compared to Z/D. In the area where the model holds, a value of ε_p was calculated at each point (X/D, Z/D). The arithmetic mean of these values (about 100 points) was then calculated. These values of $\bar{\varepsilon}_p$ for each value of M and U_∞ are shown on Figure 4.

At high values of the blowing rate, the jet penetrates into the free stream and has little influence on the wall temperature. Equation 10 was then used to obtain ε_p from each of the centerline temperature profiles in Reference 7

at four axial locations (X/D = 1.87, 3.56, 5.48, and 10.57) where profiles were measured for each value of M and U_∞. Values of $\bar{\varepsilon}_p$ calculated with this procedure are also shown in Figure 4.

The effective turbulent diffusivity is seen to increase with the blowing rate M. It can be observed that at the same values of U_∞ and M (M = 0.1 and U_∞ = 60.6 m/s or M = 0.5 and U_∞=30.3 m/s) agreement between the diffusivities obtained by the two methods is quite good. Figure 5 greatly reduces the dependence on free stream velocity by presenting $\bar{\varepsilon}_p$ in dimensionless form. The quantity $\bar{\varepsilon}_p/U_\infty D$ used in this figure is the inverse of the Peclet number with the molecular thermal diffusivity replaced by the effective turbulent diffusivity.

Using the values of Y_o/D and $\bar{\varepsilon}_p$ from Figures 3 and 4 and Equation 8, some temperature profiles were predicted and compared with measured profiles from Reference 7. The experimental points and calculated lines are shown for blowing rates M = 0.10, 0.51, 0.99, and 2.01 on Figures 6-9 respectively. The profiles are located in the centerline plane (Z/D = 0) and at four different downstream locations.

Positioning the source a distance Y_o/D above the point of injection has the effect of moving the peak of the temperature profile away from the wall and into the flow at the higher blowing rates. Agreement between the model's predictions

and the experimental data is good at the low blowing rates, as was already demonstrated in Reference 2, and at the downstream stations for the higher blowing rates.

Predicted and measured values of the film cooling effectiveness at blowing rates M = 0.10, 0.51, and 1.00 are shown in Figures 10-12. The blowing rate M = 2.0 is not included since both measured and predicted values of η are very small. The experimental values of the film cooling effectiveness are taken from Reference 6. The lines were calculated with Equation 8 using values of Y_o/D from Figure 3 and the effective turbulent diffusivity for the point source model from Figure 4. The dependence of the film cooling effectiveness upon the distance X/D downstream of injection is shown at several lateral positions in the lower part of each figure. The curves exhibit the desired shape except for the region immediately downstream of injection, and agreement between the model and experimental results is good along the centerline (Z/D = 0.0). Better agreement close to the injection location might be obtained by removing the assumption that X is large (made following Equation 4) and using the resulting equation which would replace Equation 8. Agreement is not as good at locations off the centerline. The predicted values of the film cooling effectiveness are usually low at these lateral positions.

The plots in the upper right corner of each figure, where the film cooling effectiveness is shown as a function of the lateral position Z/D at several downstream locations, point this difference out more clearly. The temperature distribution resulting from the point source is too narrow. This is obviously a consequence of the fact that the energy released through the hole in the experiments is distributed over an area of one diameter width, whereas the point energy source has no width at X/D = 0.

In summary, it can be concluded that a single value of the distance Y_o and of the turbulent diffusivity $\bar{\varepsilon}_p$ over the area used in this section describes the trends in the development of the temperature field and in the effectiveness qualitatively quite well. If a more accurate quantitative prediction is desired, then the parameters Y_o and ε_p have to be determined over a narrower area. Equation 8 with these values then constitutes an interpolation formula for the respective area.

The Line Source Model

As with point source model, it is necessary to determine the distance the source lies above the wall and the effective turbulent diffusivity before the model can be applied. The distance Y_o/D from the line source to the wall is assumed to be identical to that used for the point source (see Figure 3).

Data from Reference 6 were used to obtain the diffusivity $\bar{\varepsilon}_\ell$ and the procedure was the same as that used for a point source, only now Equation 15 was applied. Again, the convergence scheme did not converge in the area where X/D is not large compared to Z/D. The numerical average of the individual values of ε_ℓ (about 100 points) was calculated in the area where the model holds. These values of $\bar{\varepsilon}_\ell$ are shown for each value of M and U_∞ in Figure 13. At high values of the blowing rate, it was again necessary to use maximum temperatures measured in the flow to determine ε_ℓ from Equation 15. The results of this calculation are included in Figure 13. Agreement between the results of the two methods of determining $\bar{\varepsilon}_\ell$ at the same values of U_∞ and M is again good. The values of the effective turbulent diffusivity $\bar{\varepsilon}_\ell$ for the line source model are slightly less than the values $\bar{\varepsilon}_p$ for the point source model. Figure 14 shows the inverse of the Peclet number based on the effective turbulent diffusivity $\bar{\varepsilon}_\ell$.

Using values of Y_o/D from Figure 3 and $\bar{\varepsilon}_\ell$ from Figure 13, the line heat source model was used to predict some of the experimental temperature profiles from Reference 7. The experimental points and calculated lines are shown on Figures 15-18 for blowing rates M = 0.10, 0.51, 0.99, and 2.01. The profiles are located in the plane Z/D = 0 and at four different downstream locations X/D. The calculated profiles have the same shape as those that were calculated for the point source

since the functional form of the equations for the point source (Equation 8) and line source (Equation 15) is the same with respect to Y/D. Because the values of $\bar{\varepsilon}_{\ell}$ are lower than the values of $\bar{\varepsilon}_{p}$, the calculated temperature profiles (at Z/D = 0) for the line source do not agree as well with the experimental profiles as those for the point source at blowing rates M = 0.10 and 0.51. There is only a slight difference between the two sets of calculated profiles at the blowing rates M = 0.99 and 2.01.

Figures 19-21 present comparisons of experimental values of the film cooling effectiveness of Reference 6 and values predicted by the line source model at blowing rates M = 0.10, 0.51, and 1.00. The blowing rate M = 2.0 is not included since both measured and predicted values of the film cooling effectiveness are very small. Again values of Y_o/D from Figure 3 and values of $\bar{\varepsilon}_{\ell}$ from Figure 13 were used in the calculation. There is some improvement in the off-centerline values of the film cooling effectiveness predicted by the line source model over those predicted by the point source model. It is, however, questionable whether the improvement warrants the use of the line wource model over the point source.

Various other adjustments of the energy source model suggest themselves. Better agreement on lateral spreading may be obtainable by a model consisting of two point sources arranged at a distance D apart at X = 0 and Z = $\pm$ D/2. The

local variation of the turbulent diffusivity in the boundary layer could be included by an empirical adjustment of Equation 8, leading to equations similar to those in References 4 and 5. One might also try to use the centerline of the actual jet (the location of the maximum temperature T_m) for the centerline of the temperature field resulting from the energy source. Effects of the boundary layer thickness at the point of injected fluid would then enter the model through their effect on the trajectory of the jet. This, however, would require knowledge of the jet centerline which generally is not available. It is suspected that all these adjustments will not lead to an essential improvement of the results obtained with the various models.

Some effort was also spent in developing an empirical equation by statistically requiring best agreement of such an equation with the experimental results. Even expressions of a fairly complicated nature could not represent these results with a higher accuracy than the point source model. This is obviously due to the complicated nature of the interaction and of the mixing of the secondary fluid jet with the turbulent boundary layer at larger values of the blowing parameter M.

It is, therefore, felt that the best procedure for design calculations is to use the experimental information on film cooling parameters as it is contained in the literature and

as it will become available in the future and to interpolate between the experimental data by the equations derived from the point heat source model with values of Y_o and ε_p determined in the area of interpolation. For rows of holes or for interrupted slots, use should be made of the superposition principle to adjust the interpolation formula to this condition, though care must be taken due to the interaction of jets, particularly far downstream.

VI. CONCLUSIONS

1. The point energy source model of Reference 2 can be adapted to describe film cooling with ejection through a circular hole at large blowing rates by locating the source some distance above the film cooled surface.
2. Use of a line energy source with a length equal to the diameter of the hole somewhat improves the agreement between the temperature field and effectiveness calculated with the model and experimental results obtained for ejection of the secondary fluid through a hole.
3. For closer quantitative agreement it is suggested that the relations obtained from the energy source models be used as interpolation formulas upon determining the distance of the source above the wall and the turbulent diffusivity from experimental information in the area close to the desired location.

ACKNOWLEDGMENTS

The authors wish to express their appreciation to P. R. Glamm for his aid during the course of the investigation.

BIBLIOGRAPHY

1. E.R.G. Eckert, "Transpiration and Film Cooling," in Heat Transfer Symposium, University of Michigan Press, 1953.

2. J.W. Ramsey, R.J. Goldstein, and E.R.G. Eckert, "A Model for Analysis of the Temperature Distriubtion with Injection of a Heated Jet into an Isothermal Flow," Heat Transfer 1970, Elsevier Publishing Co., Amsterdam, Netherlands, 1970.

3. H.S. Carslaw and J.C. Jaeger, Conduction of Heat in Solids, Oxford University Press, London, pp. 266-267, 1959.

4. K. Wieghardt, "Uber Ausbreitungsvorgänge in Turbulenten Reibungsshichten," A. Agnew, Math. Mech. 28 No. 11-12, pp. 346-355, 1948.

5. R.C. Malhotra and J.E. Cermak, "Mass Diffusion in Neutral and Unstably Stratified Boundary-Layer Flows," Int. J. Heat Mass Transfer, 7, pp. 169-186, 1964.

6. R.J. Goldstein, E.R.G. Eckert, and J.W. Ramsey, "Film Cooling with Injection Through a Circular Hole," NASA Cr-54604, May, 1968; (Trans. ASME, Series A, Vol 90

7. J.W. Ramsey, and R.J. Goldstein, "Interaction of a Heated Jet with a Deflecting Stream," NASA CR-72613, April, 1970; (University of Minnesota, HTL TR No. 92).

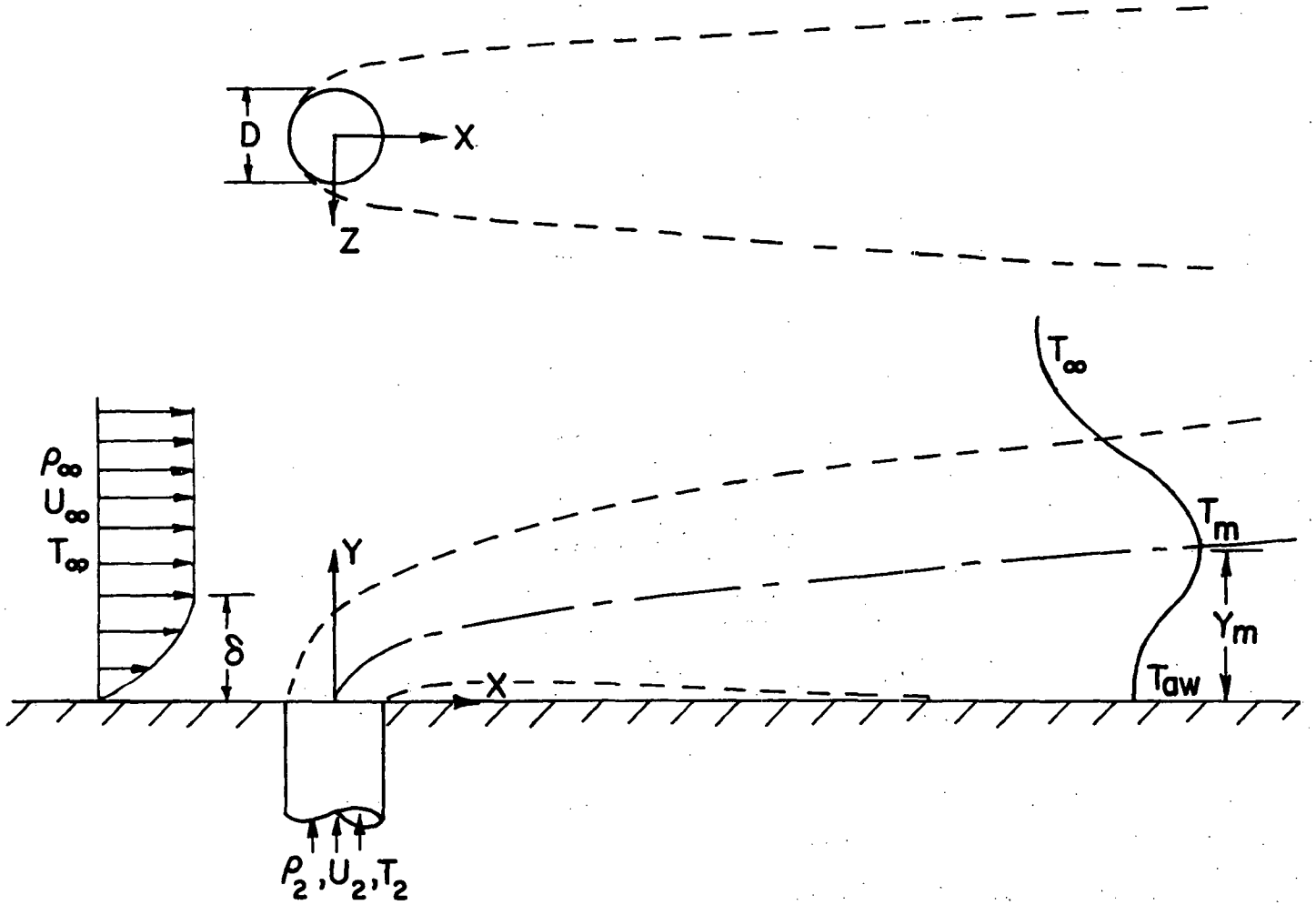

Figure 1 - Circular jet injected normal to a crossflow

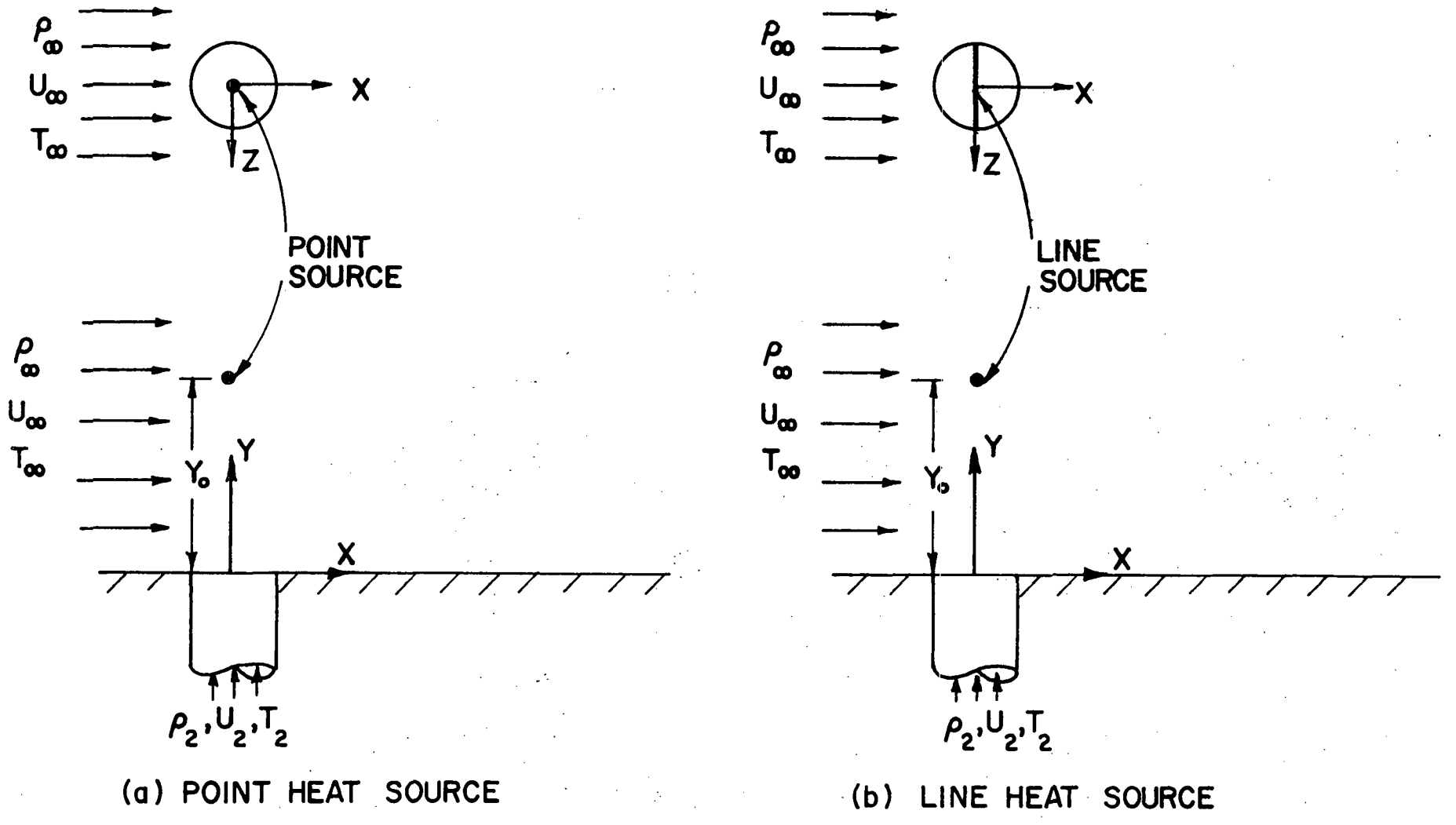

Figure 2 - Location of point and line source models in the crossflow

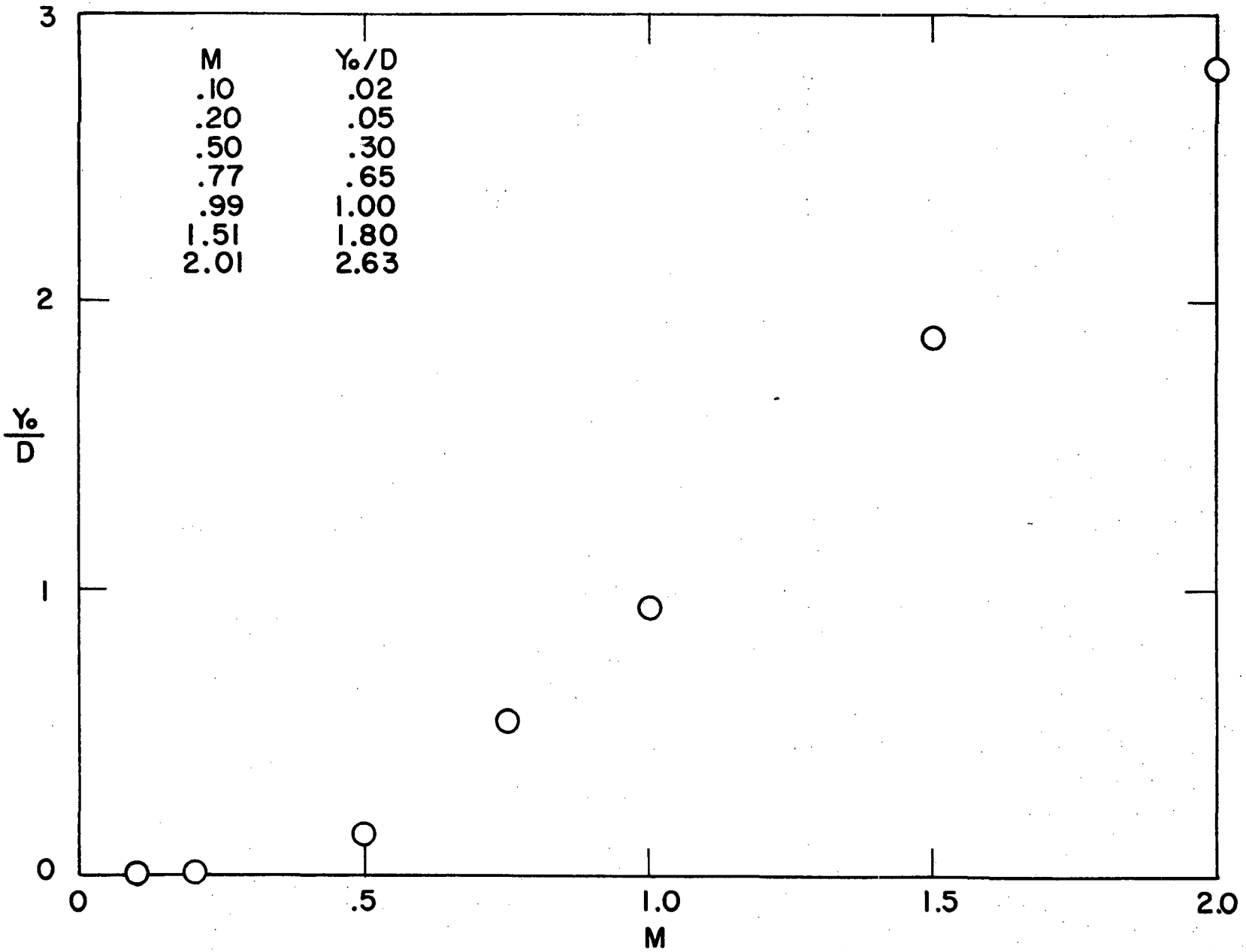

Figure 3 - Average penetration of a jet injected normal to a crossflow

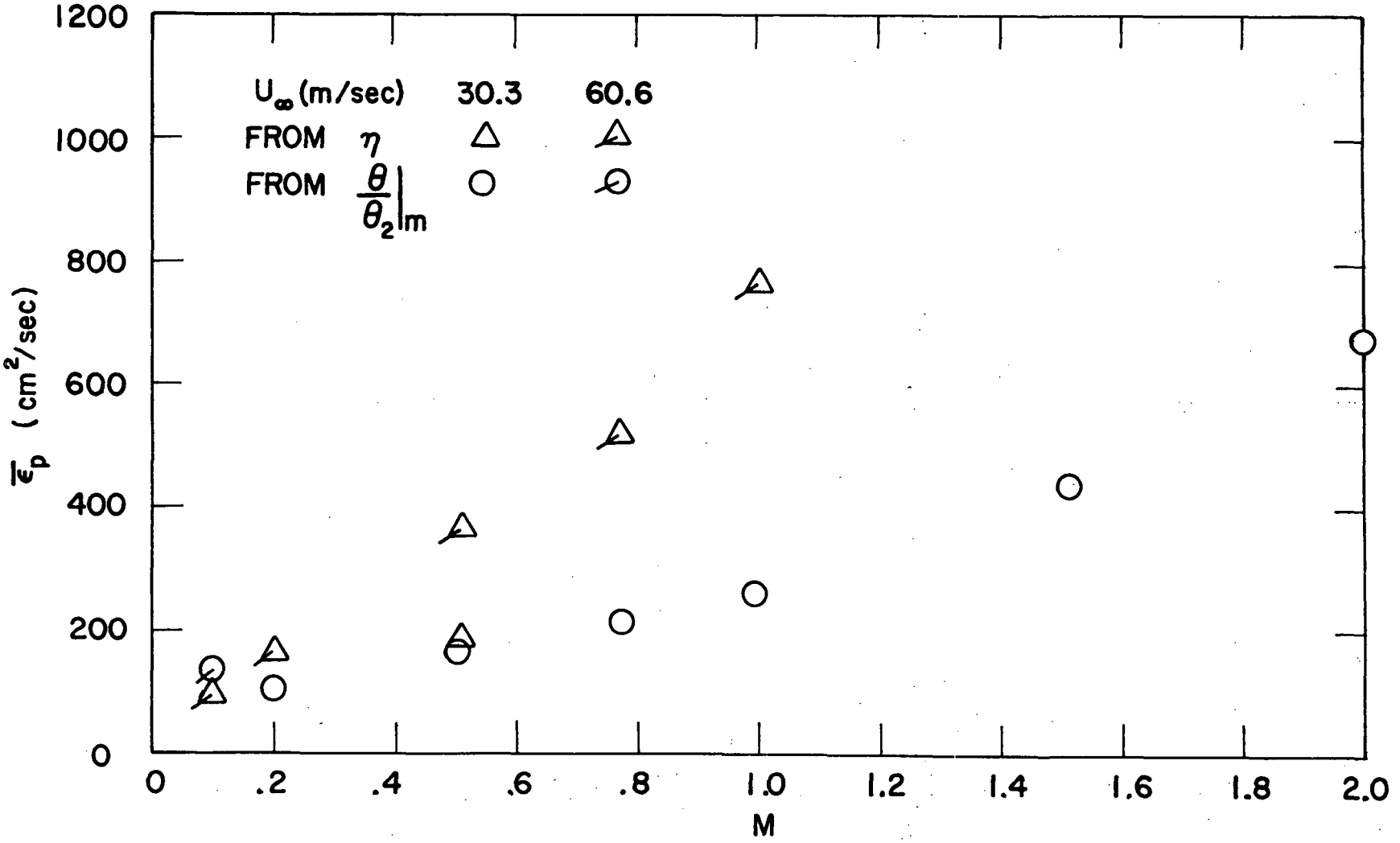

Figure 4 - Average effective turbulent diffusivity for a point source

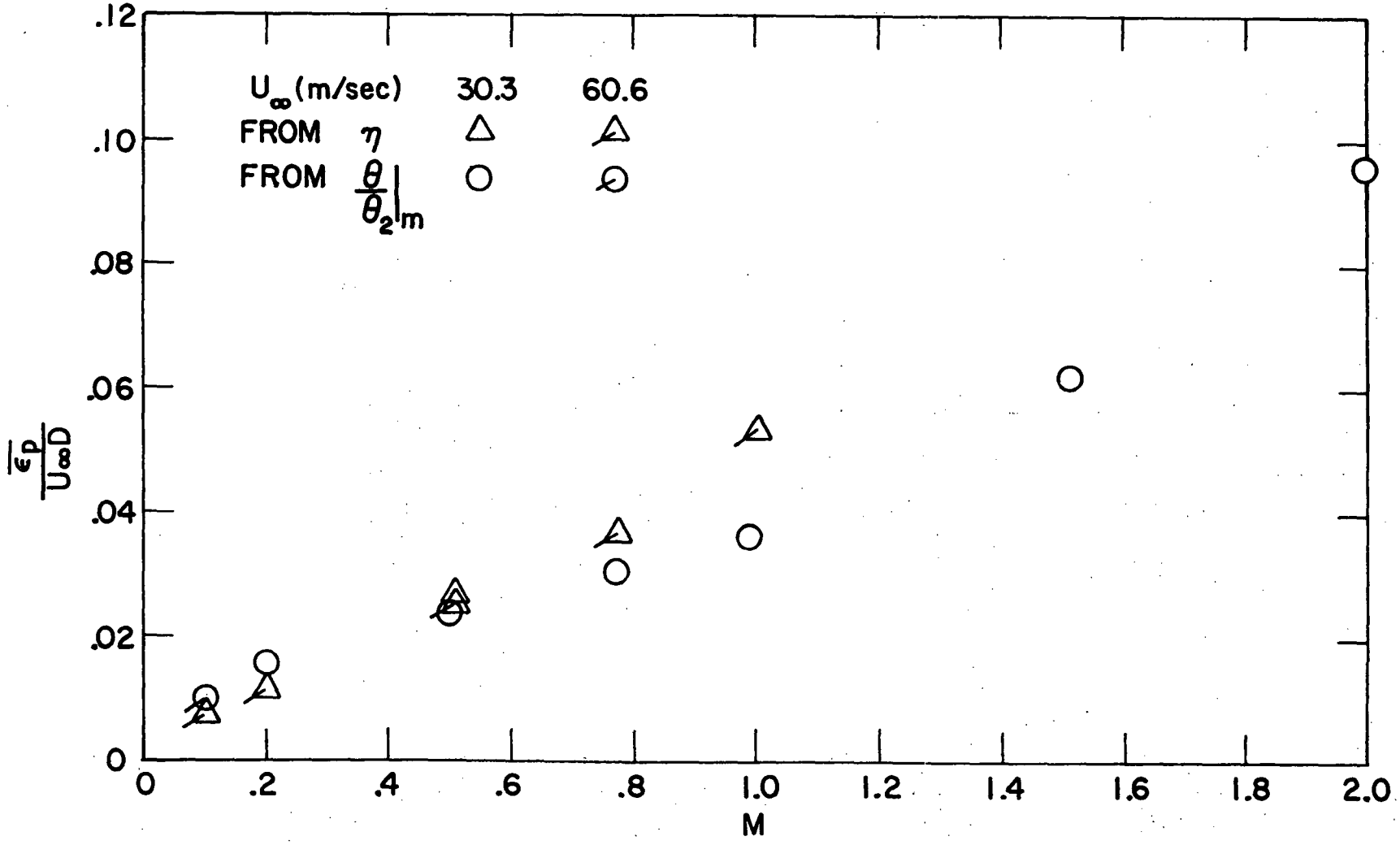

Figure 5 - Dimensionless average effective turbulent diffusivity for a point source

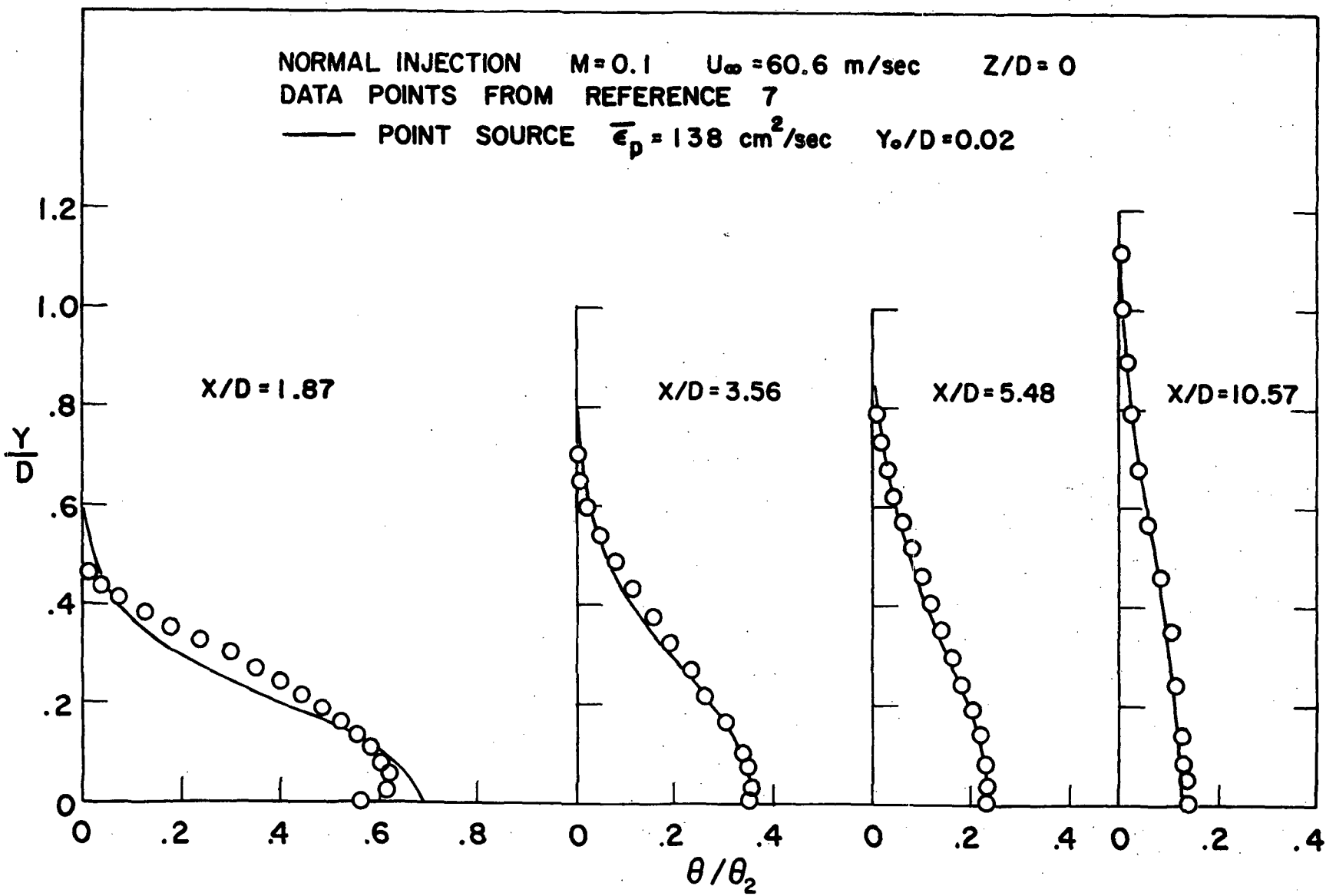

Figure 6 - Comparison of temperature profiles predicted by point source model with experimental results

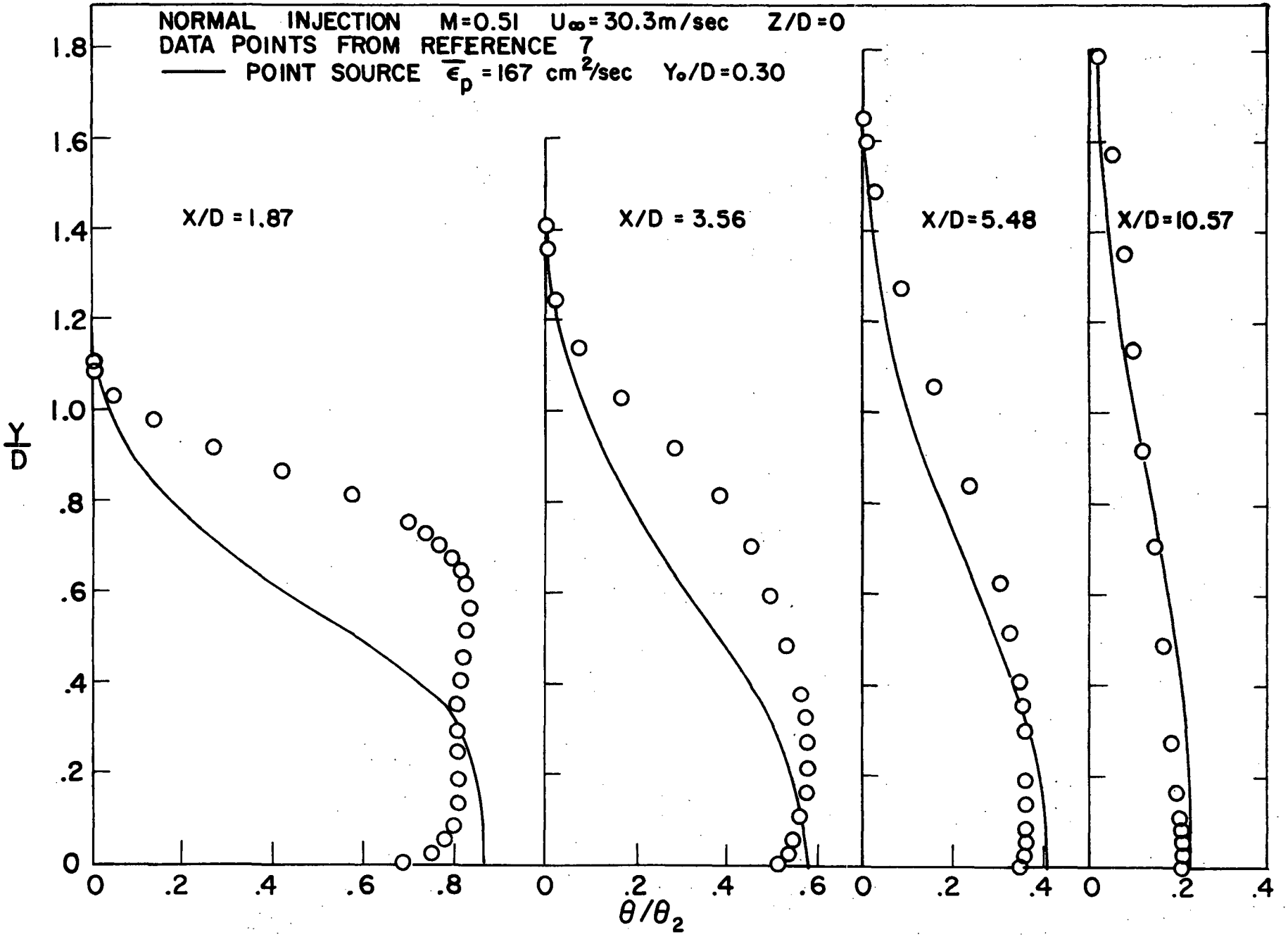

Figure 7 - Comparison of temperature profiles predicted by point source model with experimental results

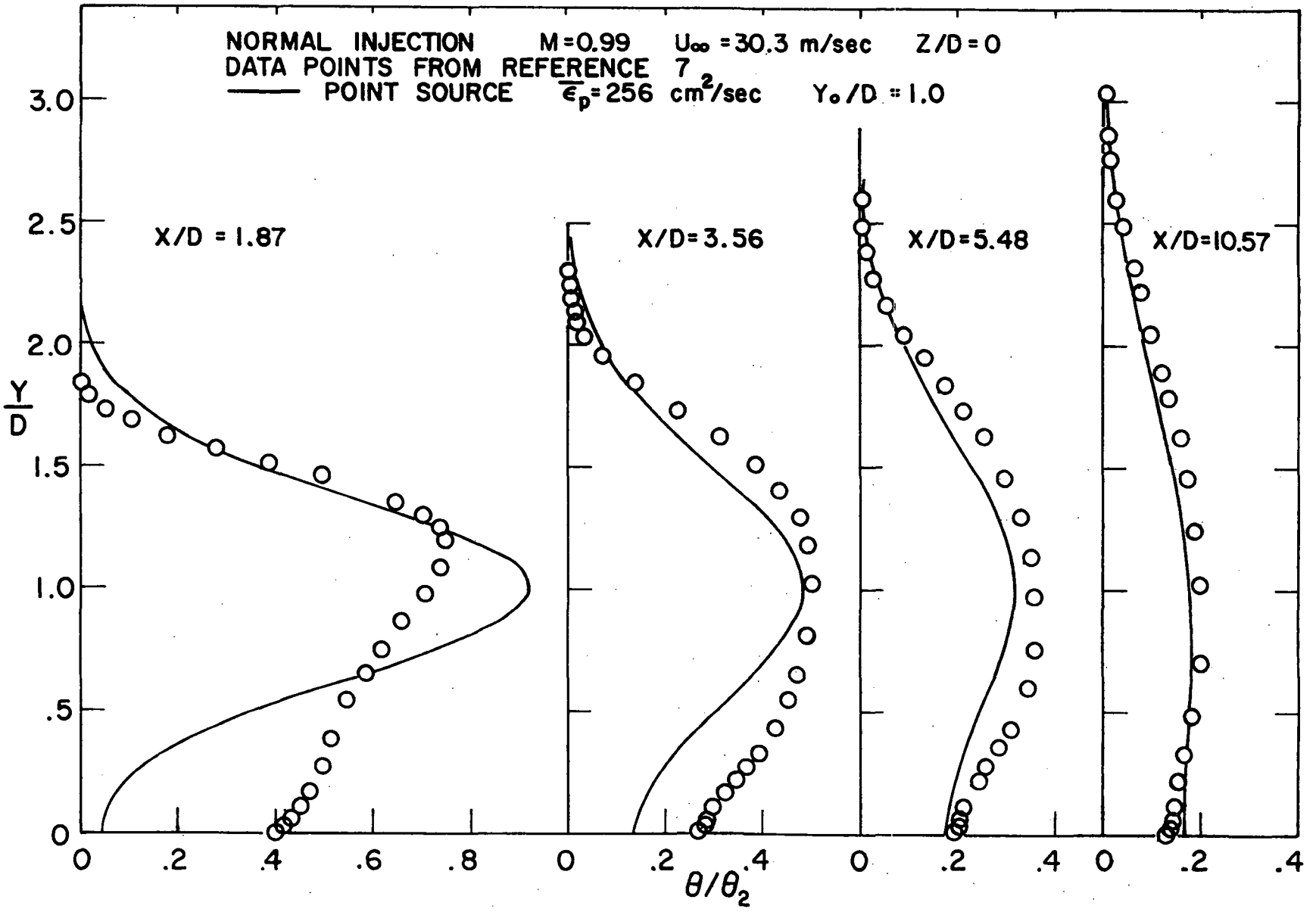

Figure 8 - Comparison of temperature profiles predicted by point source model with experimental results

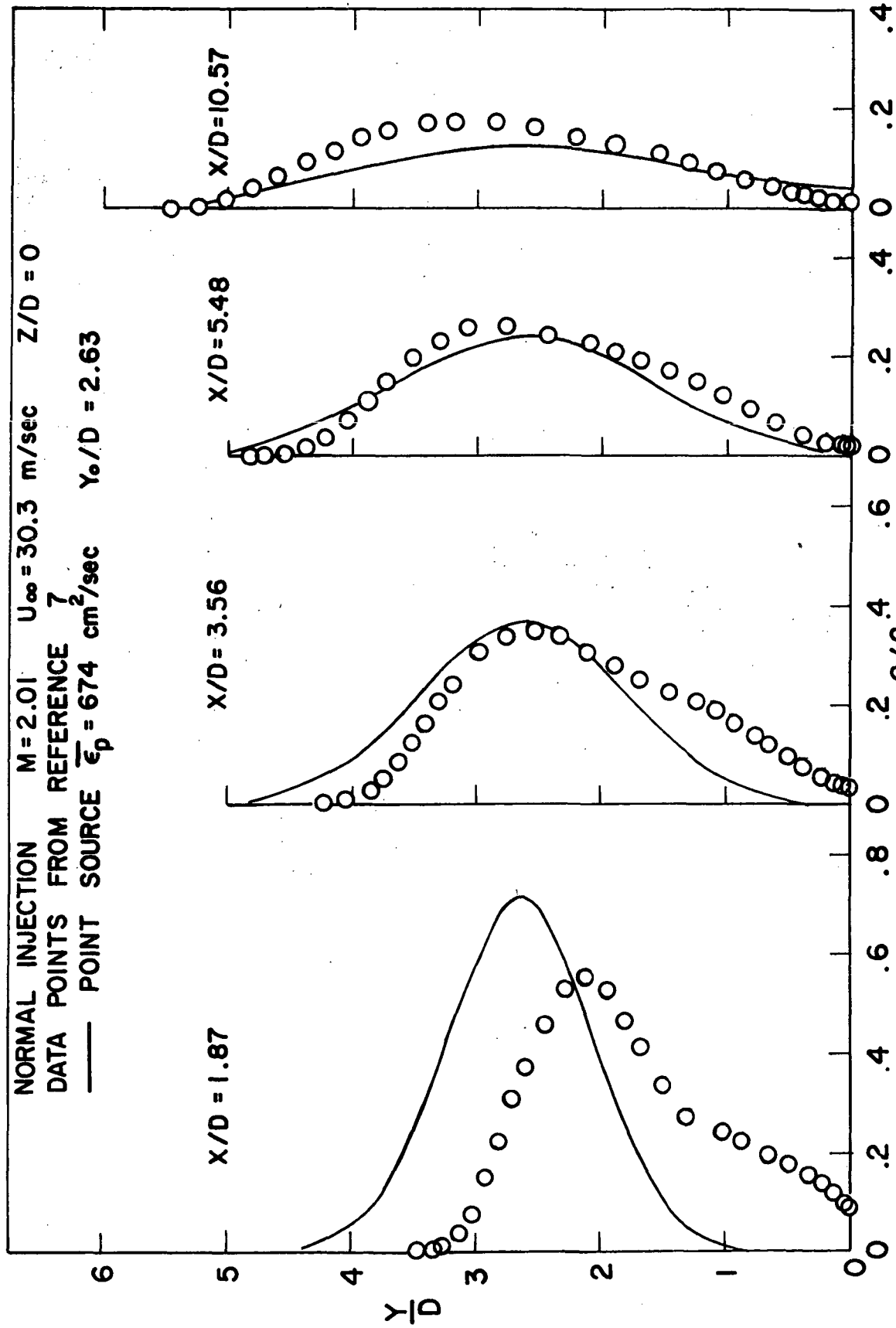

Figure 9 - Comparison of temperature profiles predicted by point source model with experimental results

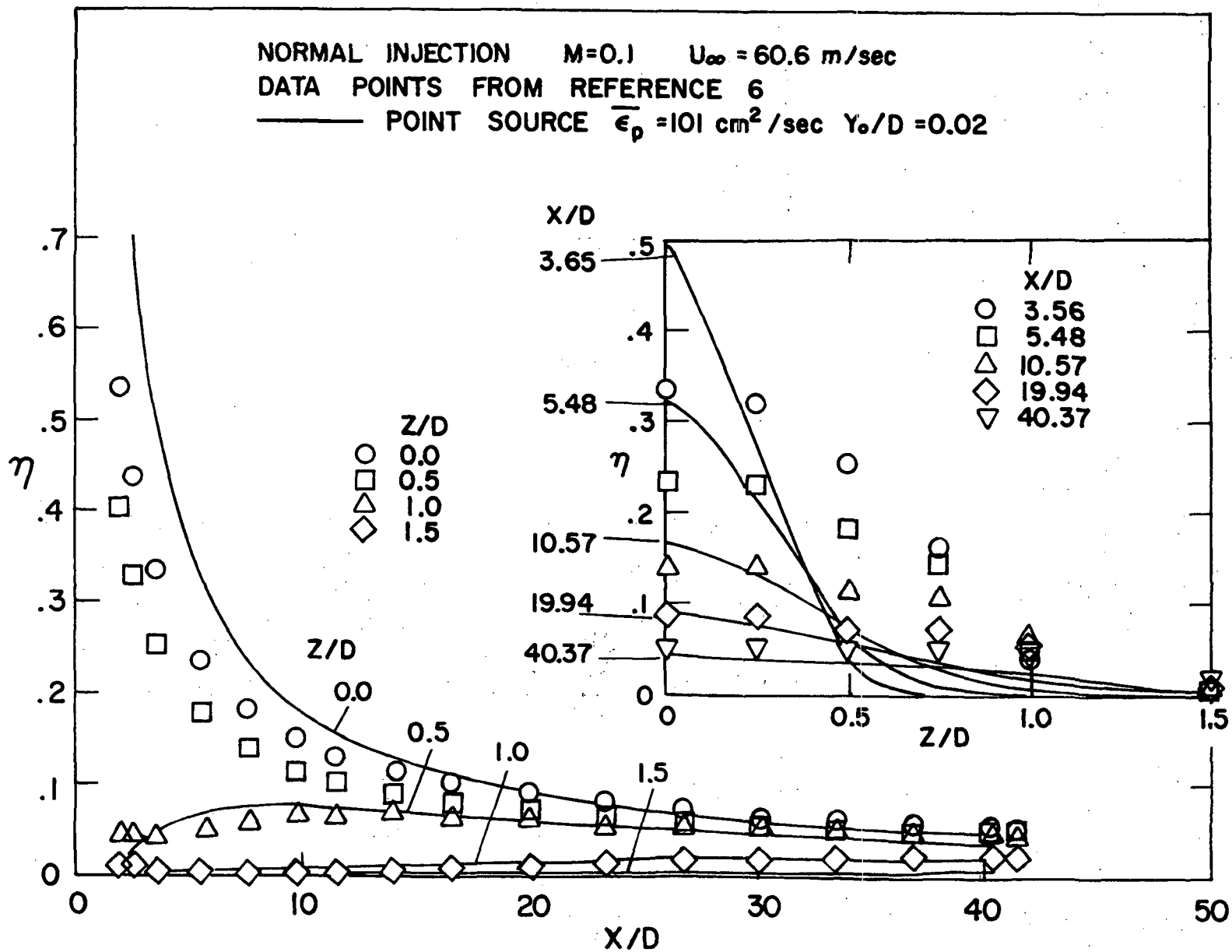

Figure 10 - Comparison of film cooling effectiveness predicted by point source model with experimental results

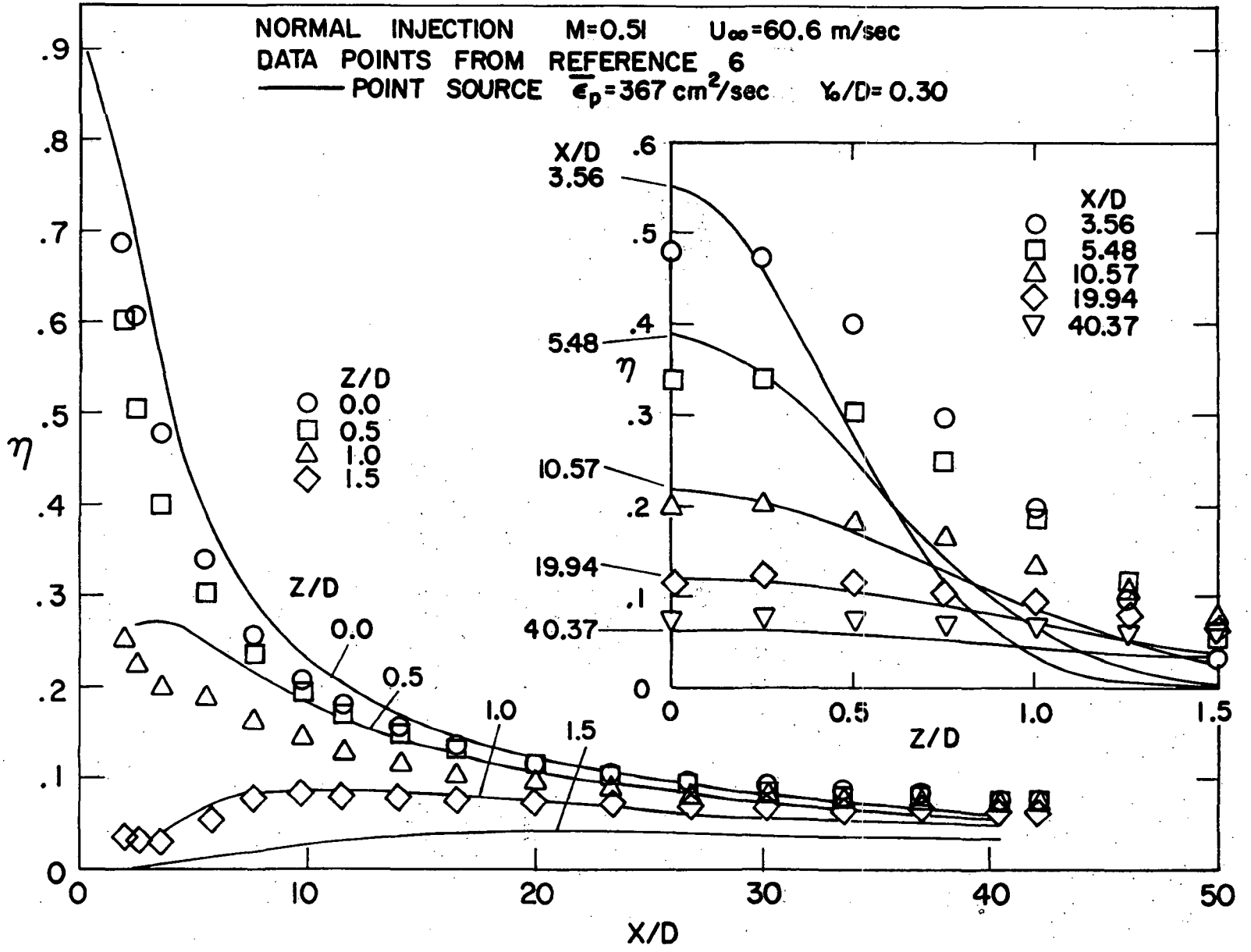

Figure 11 - Comparison of film cooling effectiveness predicted by point source model with experimental results

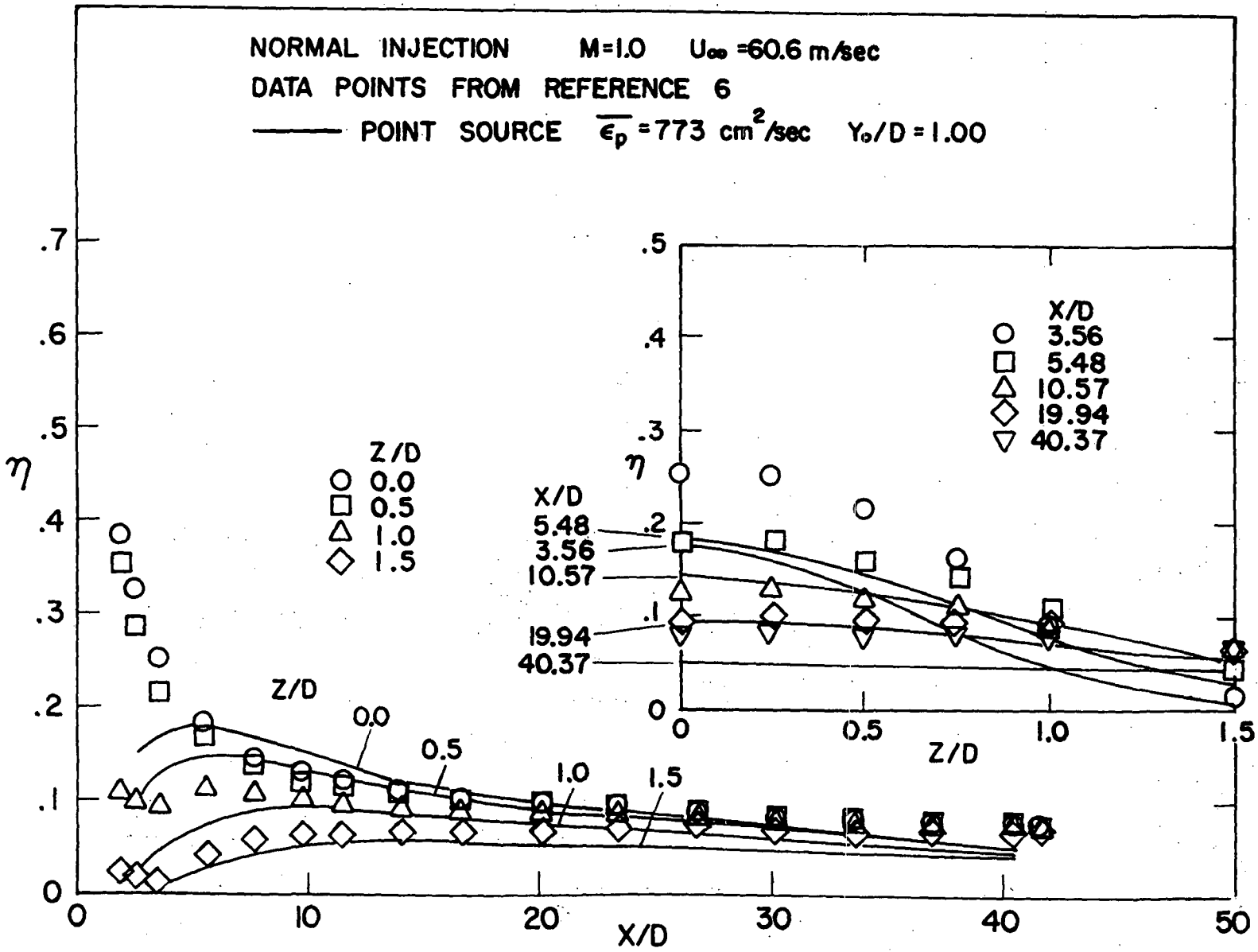

Figure 12 - Comparison of film cooling effectiveness predicted by point source model with experimental results

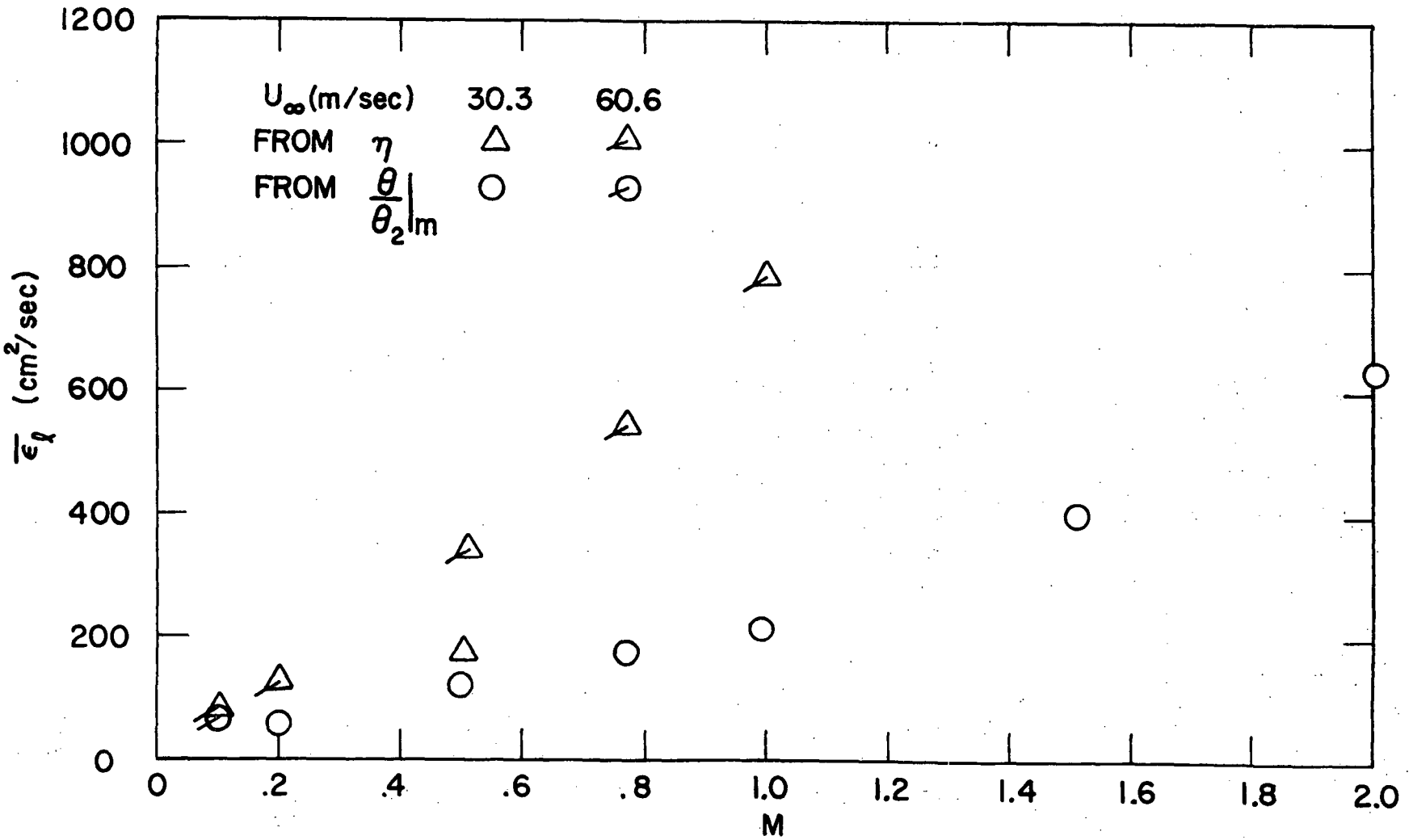

Figure 13 - Average effective turbulent diffusivity for a line source

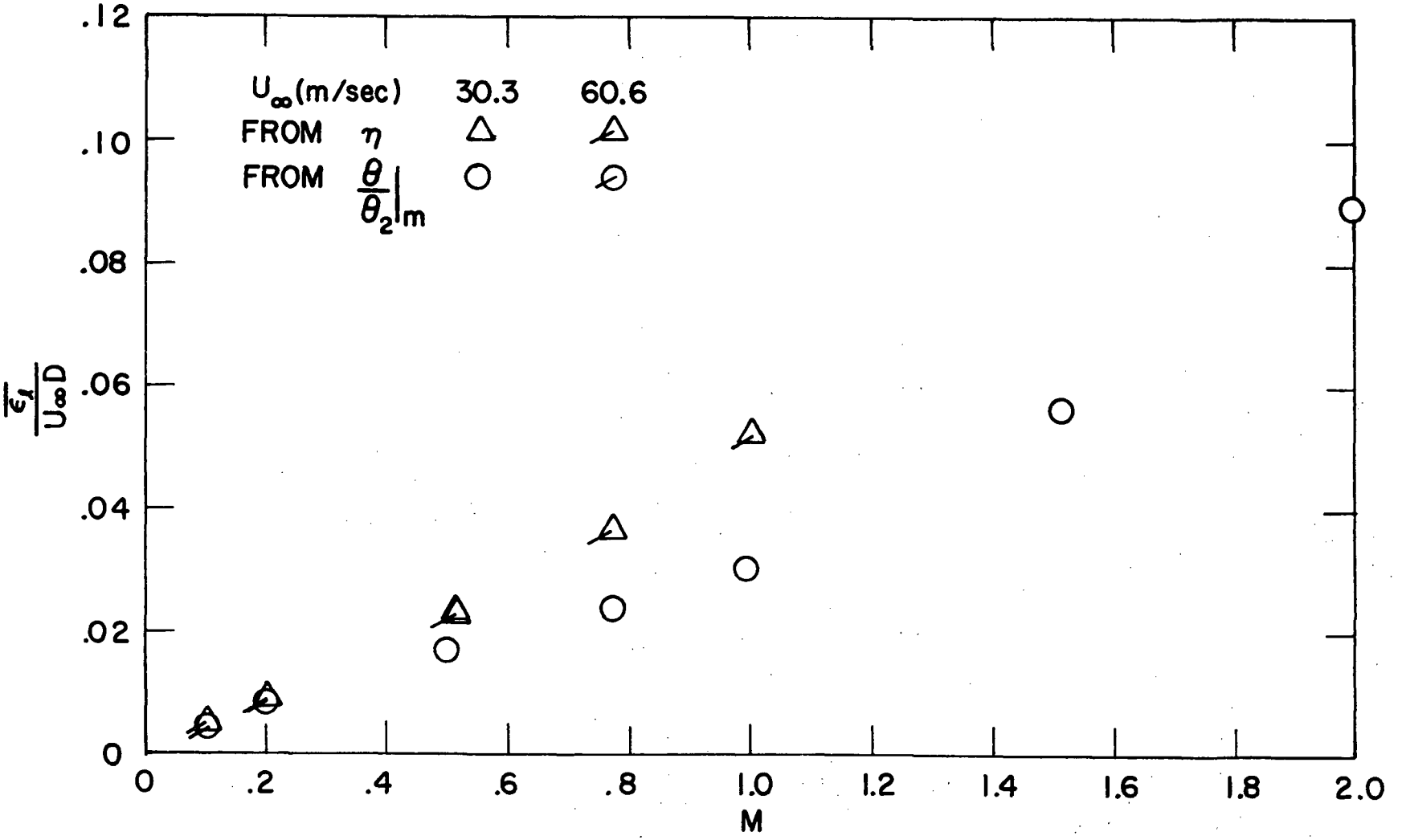

Figure 14 - Dimensionless average effective turbulent diffusivity for a line source

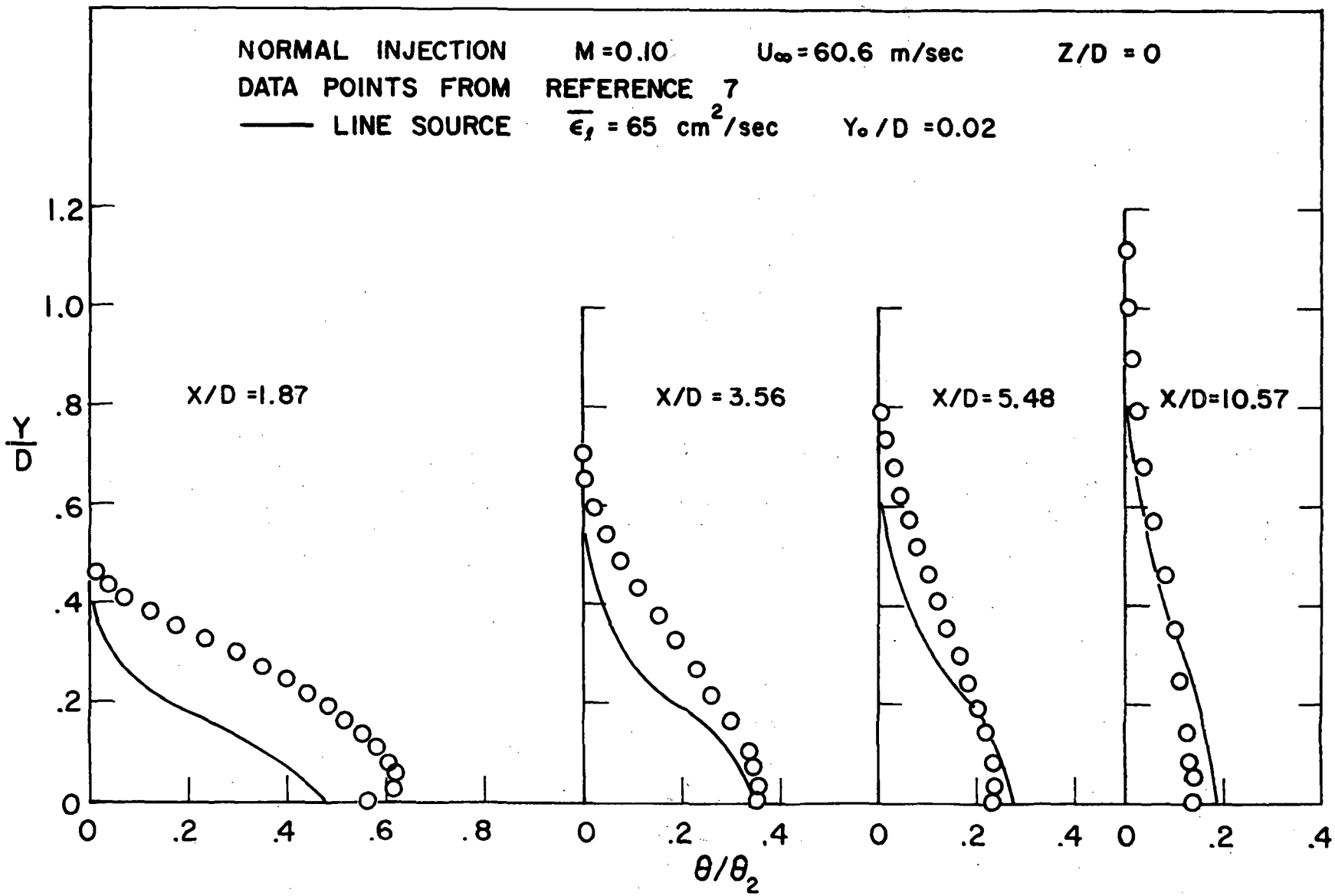

Figure 15 Comparison of temperature profiles predicted by line source model with experimental results

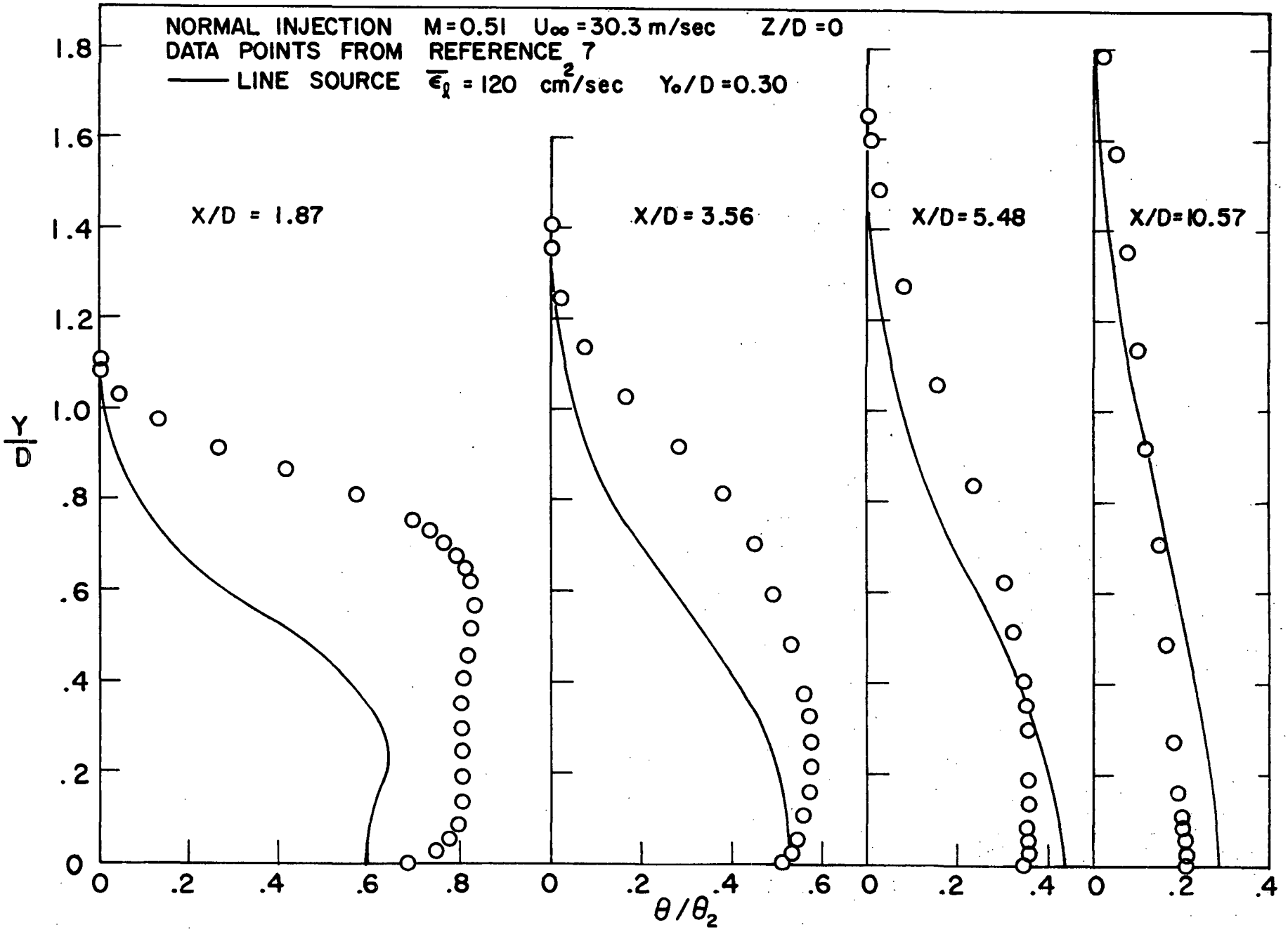

Figure 16 - Comparison of temperature profiles predicted by line source model with experimental results

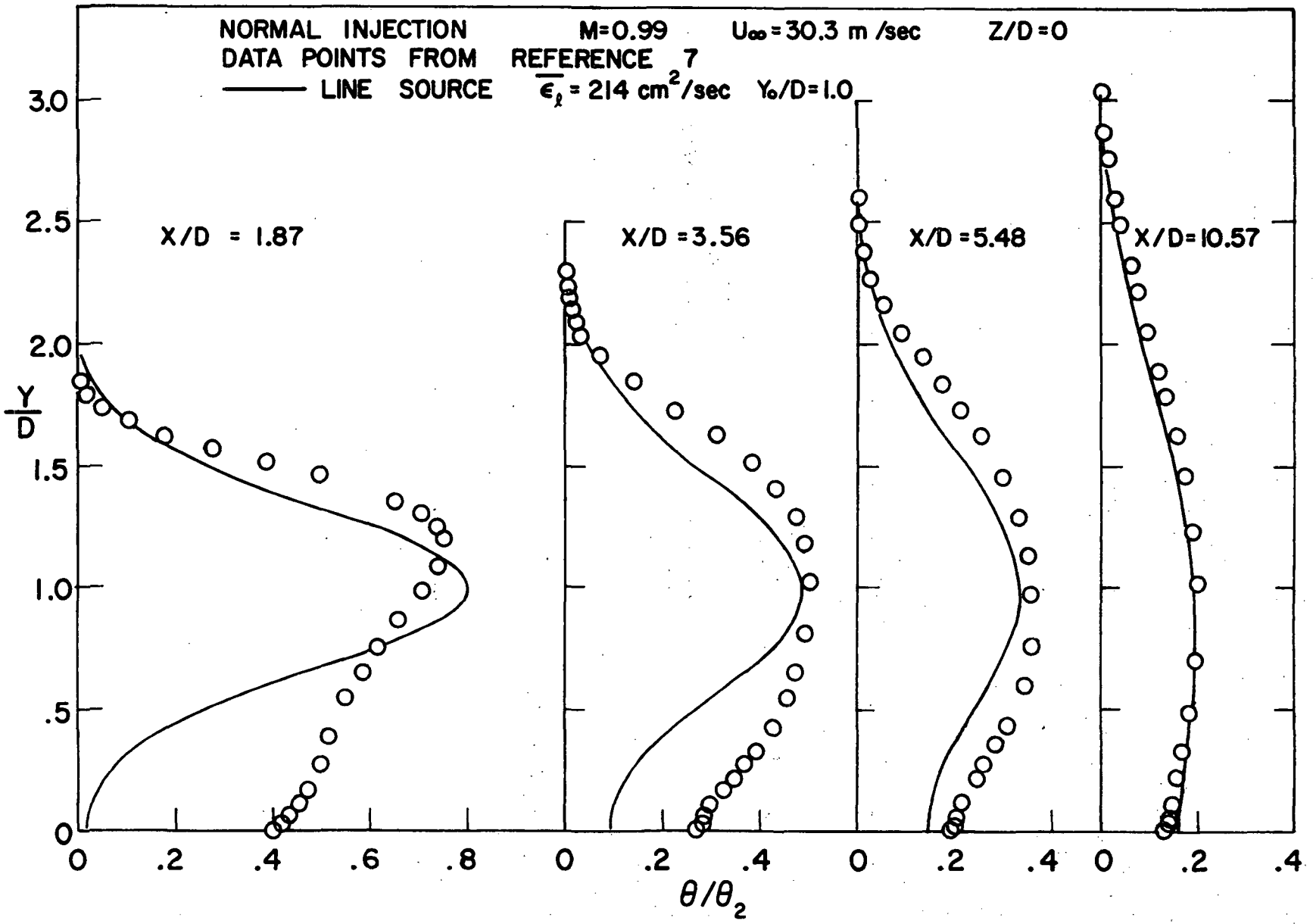

Figure 17 - Comparison of temeprature profiles predicted by line source model with experimental results

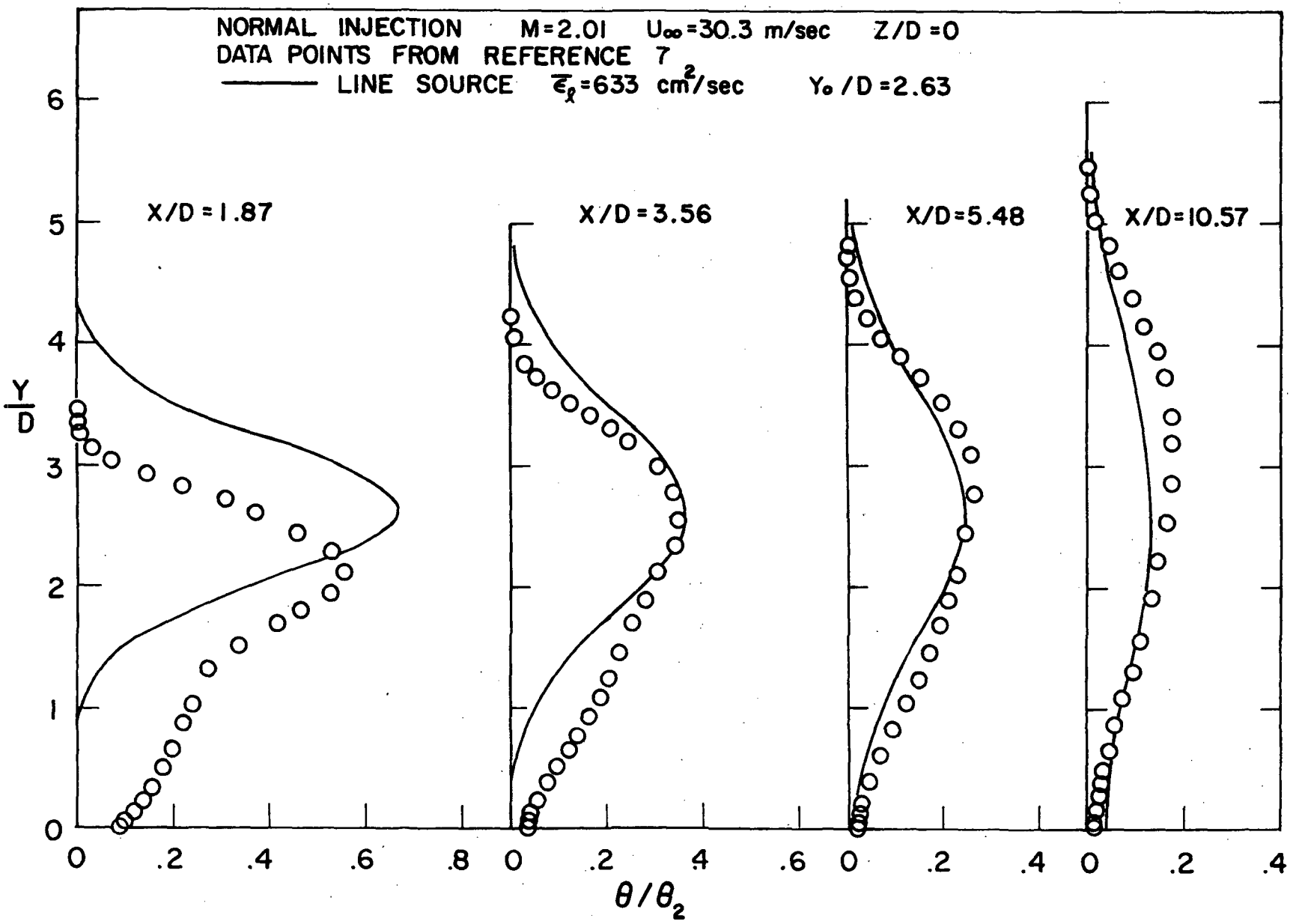

Figure 18 - Comparison of temperature profiles predicted by line source model with experimental results

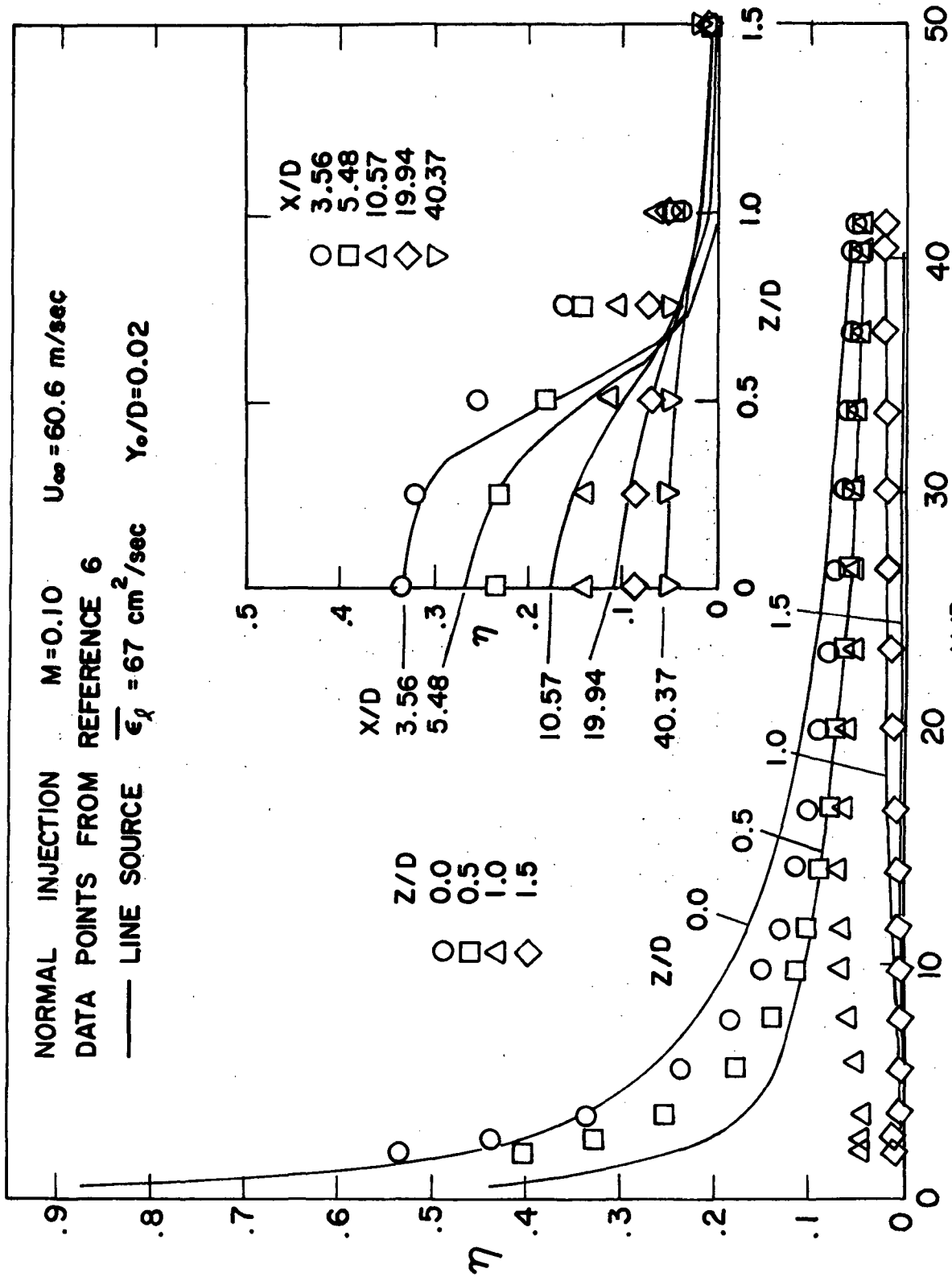

Figure 19 - Comparison of film cooling effectiveness predicted by line source model with experimental results

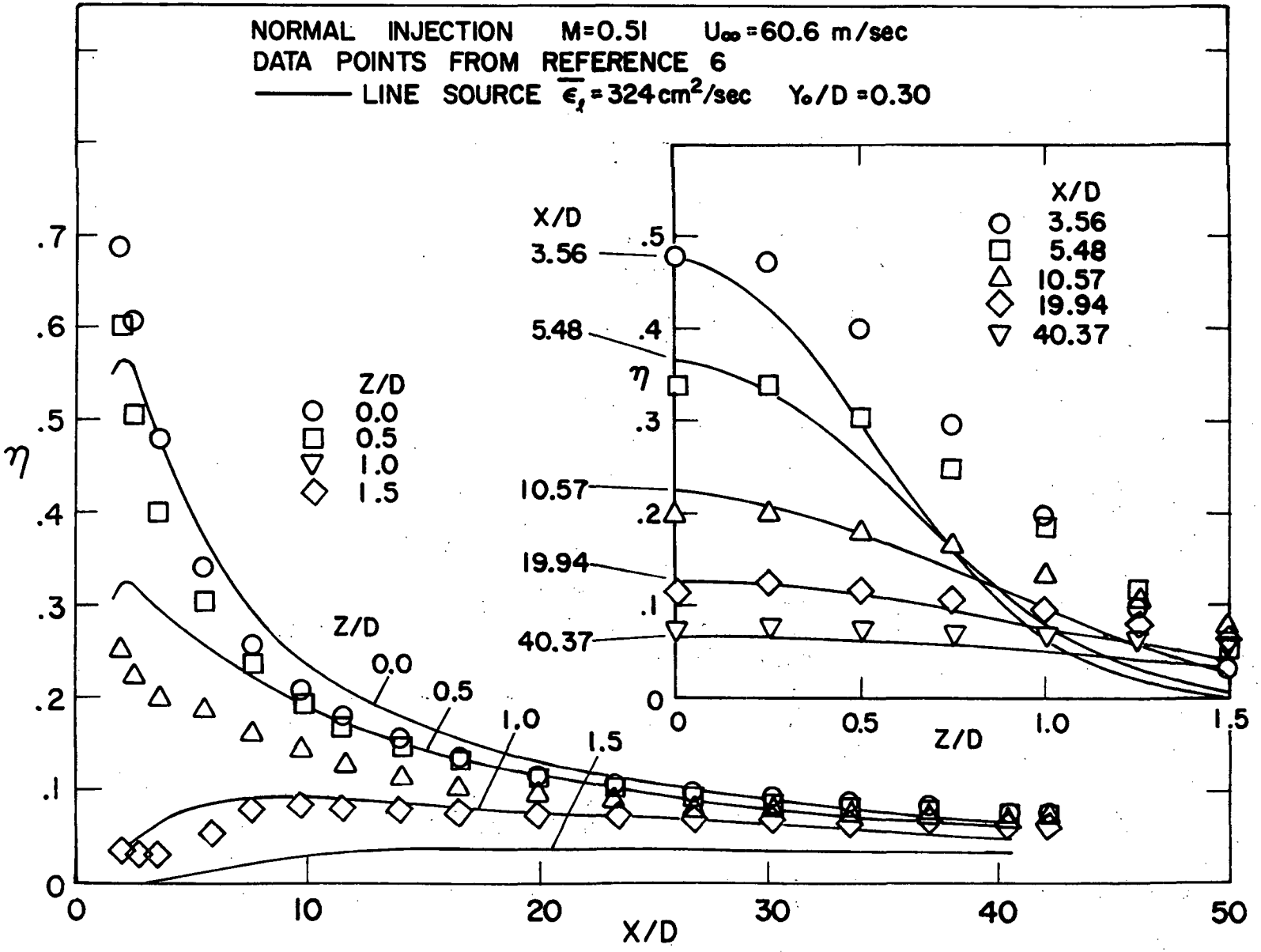

Figure 20 - Comparison of film cooling effectiveness predicted by line source model with experimental results

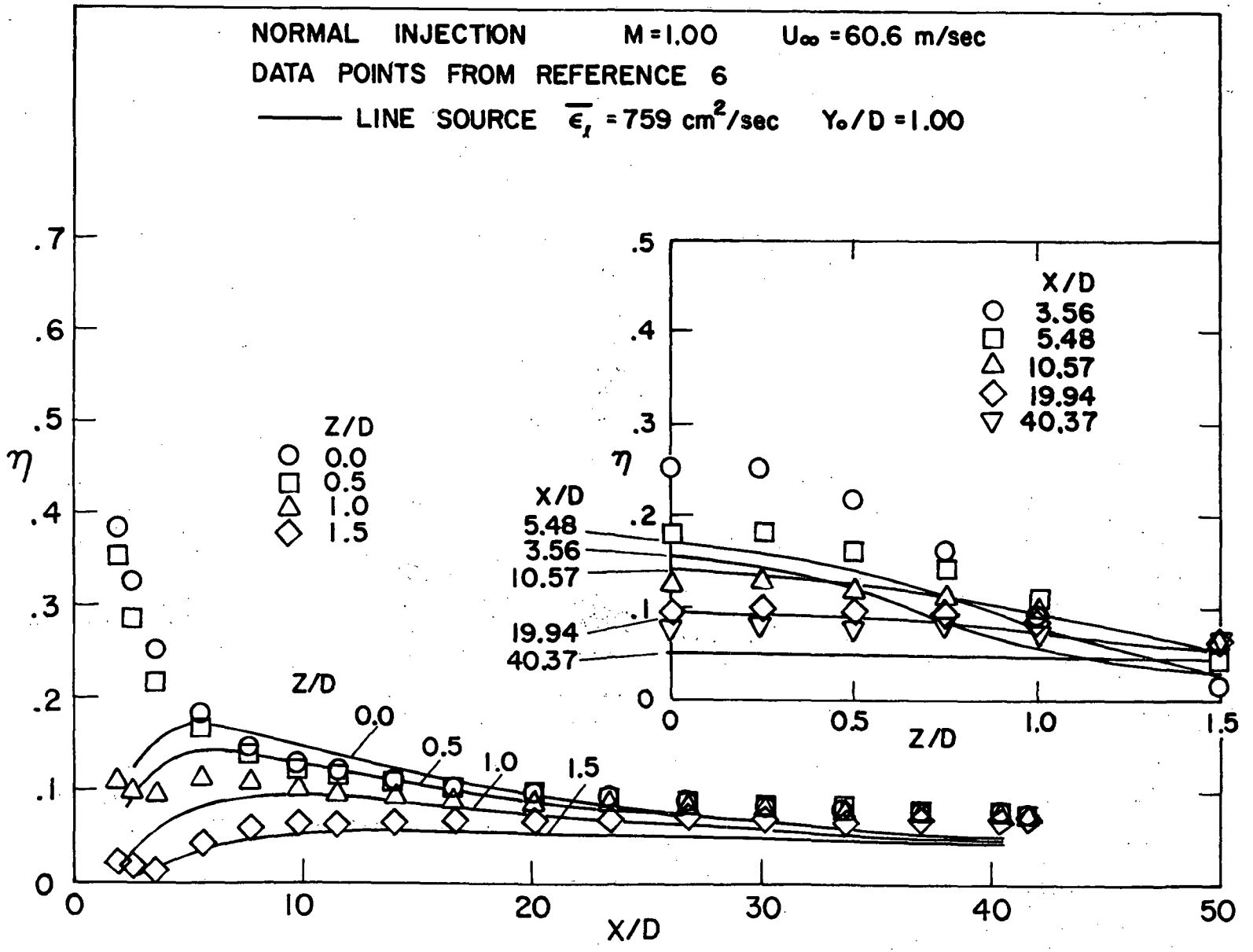

Figure 21 - Comparison of film cooling effectiveness predicted by line source model with experimental results

NAS3-13200
SUMMARY REPORT
DISTRIBUTION LIST

ADDRESSEE		Mail Stop	NUMBER OF COPIES
1. NASA Lewis Research Center 21000 Brookpark Road Cleveland, Ohio 44135			
Attention:	Aeronautics Procurement Section	77-3	1
	Reports Control Office	5-5	1
	Technology Utilization Office	3-19	1
	Library	60-3	2
	Fluid System Components Div.	5-3	1
	B. Lubarsky	3-3	1
	J. Howard Childs	60-4	1
	J. B. Esgar	60-4	1
	F. S. Stepka	60-6	10
	R. S. Colladay	60-6	1
	H. Ellerbrock	60-4	6
	J. Livingood	60-6	1
2. NASA Scientific & Technical Information Facility P.O. Box 33 College Park, Maryland 20740 Attention: NASA Representative RQT-2448			6
3. Dr. W. Kays Stanford University Stanford, California 94305			1
4. NASA Headquarters Washington, D.C. 20546 Attention: N. F. Rekos (RLC)			1
5. Department of the Army U.S. Army Aviation Material Laboratory Fort Eustis, Va. 23604 Attention: John White			1
6. Headquarters Wright-Patterson AFB, Ohio 45433 Attention: Jack Richens	(AFAPL/APTC)		2
7. Air Force Office of Scientific Research Propulsion Research Division USAF Washington, D.C. 20025			1

8. Defense Documentation Center (DDC)
Cameron Station
5010 Duke Street
Alexandria, Virginia 22314 — 1

9. NASA-Langley Research Center
Langley Station
Technical Library
Hampton, Virginia 23365
Attention: Mark R. Nichols — 1
John V. Becker — 1

10. United Aircraft Corporation
Pratt & Whitney Aircraft Division
Florida Research & Development Center
P.O. Box 2691
West Palm Beach, Florida 33402
Attention: R. A. Schmidtke — 1

11. United Aircraft Corporation
Pratt & Whitney Aircraft Division
400 Main Street
East Hartford, Connecticut 06108
Attention: C. Andreini — 2
Library — 1
M. Suo — 1

12. United Aircraft Research
East Hartford, Connecticut
Attention: Library — 1

13. Allison Division of GMC
Department 8894, Plant 8
P.O. Box 894
Indianapolis, Indiana 46206
Attention: J. N. Barney — 1
C. E. Holbrook — 1
Library — 1

14. Northern Research & Engineering Corporation
219 Vassar Street
Cambridge, Massachusetts
Attention: K. Ginwala — 1

15. General Electric Company
Flight Propulsion Division
Cincinnati, Ohio 45125
Attention: J. W. McBride — N-44 — 1
F. Burggraf — H-32 — 1
S. N. Suciu — H-32 — 1
Technical Information Center — N-32 — 1

16. General Electric Company
1000 Western Avenue
West Lynn, Massachusetts 01905
Attention: Dr. C. W. Smith--Library Bldg. 2-40M 1

17. Curtiss-Wright Corporation
Wright Aeronautical Division
Wood-Ridge, New Jersey 07075
Attention: S. Lombardo 1

18. Air Research Manufacturing Company
402 South 36th Street
Phoenix, Arizona 85034
Attention: Robert O. Bullock 1

19. Air Research Manufacturing Company
9851 Sepulveda Boulevard
Los Angeles, California 90009
Attention: Fred Faulkner 1

20. AVCO Corporation
Lycoming Division
350 South Main Street
Stratford, Connecticut 06497
Attention: Claus W. Bolton 1
Charles Kuintzle 1

21. Continental Aviation & Engineering Corporation
12700 Kercheval
Detroit, Michigan 48215
Attention: Eli H. Benstein 1
Howard C. Walch 1

22. International Harvester Company
Solar Division - 2200 Pacific Highway
San Diego, California 92112
Attention: P. A. Pitt 1
Mrs. L. Walper 1

23. George Derderian AIR 53662B
Department of Navy
Bureau of Navy
Washington, D.C. 20360 1

24. The Boeing Company
Commercial Airplane Division
P.O. Box 3991
Seattle, Washington 98124
Attention: C. J. Schott 80-66 1

25. Aerojet-General Corporation
Sacramento, California 95809
Attention: M. S. Nylin 1
Library 1
William Heath 1

26. Newark College of Engineering
323 High Street
Newark, New Jersey 07102
Attention: Dr. Peter Hrycak 1

27. Department of Mechanical Engineering
Arizona State University
Tempe, Arizona
Attention: Dr. D. E. Metzger 1